

FINITE ELEMENT ANALYSIS OF THE PLASTIC
BUCKLING OF A CANTILEVER BEAM

CENTRE FOR NEWFOUNDLAND STUDIES

**TOTAL OF 10 PAGES ONLY
MAY BE XEROXED**

(Without Author's Permission)

QIZHONG YUAN



INFORMATION TO USERS

This manuscript has been reproduced from the microfilm master. UMI films the text directly from the original or copy submitted. Thus, some thesis and dissertation copies are in typewriter face, while others may be from any type of computer printer.

The quality of this reproduction is dependent upon the quality of the copy submitted. Broken or indistinct print, colored or poor quality illustrations and photographs, print bleedthrough, substandard margins, and improper alignment can adversely affect reproduction.

In the unlikely event that the author did not send UMI a complete manuscript and there are missing pages, these will be noted. Also, if unauthorized copyright material had to be removed, a note will indicate the deletion.

Oversize materials (e.g., maps, drawings, charts) are reproduced by sectioning the original, beginning at the upper left-hand corner and continuing from left to right in equal sections with small overlaps.

Photographs included in the original manuscript have been reproduced xerographically in this copy. Higher quality 6" x 9" black and white photographic prints are available for any photographs or illustrations appearing in this copy for an additional charge. Contact UMI directly to order.

Bell & Howell Information and Learning
300 North Zeeb Road, Ann Arbor, MI 48106-1346 USA

UMI[®]
800-521-0600



National Library
of Canada

Acquisitions and
Bibliographic Services

395 Wellington Street
Ottawa ON K1A 0N4
Canada

Bibliothèque nationale
du Canada

Acquisitions et
services bibliographiques

395, rue Wellington
Ottawa ON K1A 0N4
Canada

Your file *Votre référence*

Our file *Notre référence*

The author has granted a non-exclusive licence allowing the National Library of Canada to reproduce, loan, distribute or sell copies of this thesis in microform, paper or electronic formats.

The author retains ownership of the copyright in this thesis. Neither the thesis nor substantial extracts from it may be printed or otherwise reproduced without the author's permission.

L'auteur a accordé une licence non exclusive permettant à la Bibliothèque nationale du Canada de reproduire, prêter, distribuer ou vendre des copies de cette thèse sous la forme de microfiche/film, de reproduction sur papier ou sur format électronique.

L'auteur conserve la propriété du droit d'auteur qui protège cette thèse. Ni la thèse ni des extraits substantiels de celle-ci ne doivent être imprimés ou autrement reproduits sans son autorisation.

0-612-42464-2

**FINITE ELEMENT ANALYSIS OF THE PLASTIC
BUCKLING OF A CANTILEVER BEAM**

By Qizhong Yuan, B.E.

A thesis submitted to the School of Graduate Studies
in partial fulfillment of the requirements for
the degree of Master of Engineering

Faculty of Engineering and Applied Science
Memorial University of Newfoundland

August, 1998

St. John's Newfoundland Canada

To my dear wife

ABSTRACT

Finite element analysis offers a general plastic buckling solution of structures by employing a nonlinear static plastic analysis with gradually increasing loads to seek the load level at which the structure becomes unstable. Nonlinear plastic finite element analysis requires inclusion of geometric nonlinearities and material nonlinearities in the model. Geometric nonlinearities refer to the nonlinearities in the structure due to changing geometry as it deflects. There are two kinds of geometric nonlinearities concerned in plastic buckling analysis, large strain and large deflection. On the present work, Newton-Raphson procedure, a process to solve the nonlinear equations by increasing load in several steps and iterative computation to reach the convergence criteria, is applied for the plastic buckling analysis.

A general model for rectangular cross section cantilever beams is presented, which flexibly defines the material property and dimensions of a cantilever beam. Overall behavior of the beam is studied by combining analytical methods for elastic buckling analysis and finite element analysis for plastic buckling analysis. Two non-dimensional parameter ratios of thickness by length t/l and ratio of height by thickness h/t are used to evaluate the overall behavior of a cantilever beam. The two boundaries of elastic buckling and yielding, and plastic buckling and collapse are also investigated.

ACKNOWLEDGEMENTS

I am greatly appreciative of Dr. Claude Daley, associate professor, Faculty of Engineering and Applied Science for his financial support and direction, inspiration and discussion during my master programme.

I am thankful to Dr. M.R. Haddara, Associate Dean, Faculty of Engineering and Applied Science and Dr. J.J. Sharp, former Associate Dean, Faculty of Engineering and Applied Science, their guide and assistance during the programme make the most pleasant stay in Memorial University.

I am also grateful to the school of Graduate Studies and the Faculty of Engineering and Applied Science for providing financial assistance, without which this work would not have been possible.

Sincerely thanks to my dear wife, Yuxiang Xiao, for her sacrifice, understanding, spiritual support and moral encouragement.

LIST OF FIGURES

Figure 3.1	Stress vector definition	18
Figure 3.2	Position vectors and motion of a deforming body	24
Figure 3.3	Newton-Raphson solution – one iteration	30
Figure 3.4	Newton-Raphson solution – next iteration	31
Figure 3.5	Incremental Newton-Raphson procedure	32
Figure 4.1 (a)	Nonlinear load-deflection curve	36
Figure 4.1 (b)	Linear (Eigenvalue) buckling curve	36
Figure 5.1	Cantilever beam dimensions	44
Figure 5.2	Pre-postprocessor results for $t/l=0.018$, $h/t=16$	53
Figure 5.3	Finite element results for $t/l=0.008$, $h/t=8$	56
Figure 5.4	Finite element results for $t/l=0.014$, $h/t=10$	57
Figure 5.5	Finite element results for $t/l=0.012$, $h/t=10$	58
Figure 5.6	Finite element results for $t/l=0.018$, $h/t=12$	59
Figure 5.7	Finite element results for $t/l=0.016$, $h/t=12$	60
Figure 5.8	Finite element results for $t/l=0.014$, $h/t=12$	61
Figure 5.9	Finite element results for $t/l=0.020$, $h/t=14$	62
Figure 5.10	Finite element results for $t/l=0.018$, $h/t=14$	63
Figure 5.11	Finite element results for $t/l=0.016$, $h/t=14$	64
Figure 5.12	Finite element results for $t/l=0.014$, $h/t=14$	65
Figure 5.13	Finite element results for $t/l=0.020$, $h/t=16$	66
Figure 5.14	Finite element results for $t/l=0.018$, $h/t=16$	67

Figure 5.15	Finite element results for $t/l=0.016$, $h/t=16$	68
Figure 5.16	Finite element results for $t/l=0.014$, $h/t=16$	69
Figure 5.17	Finite element results for $t/l=0.020$, $h/t=18$	70
Figure 5.18	Finite element results for $t/l=0.018$, $h/t=18$	71
Figure 5.19	Finite element results for $t/l=0.016$, $h/t=18$	72
Figure 5.20	Finite element results for $t/l=0.018$, $h/t=20$	73
Figure 5.21	Finite element results for $t/l=0.016$, $h/t=20$	74
Figure 5.22	Finite element results for $t/l=0.018$, $h/t=22$	75
Figure 5.23	Finite element results for $t/l=0.016$, $h/t=22$	76
Figure 5.24	Finite element results for $t/l=0.016$, $h/t=24$	77
Figure 5.25	Finite element results for $t/l=0.014$, $h/t=24$	78

LIST OF TABLES

Table 5.1	Analytical Boundaries	49
Table 5.2	Grid cases examined by non-linear F.E. analysis	50
Table 5.3	Comparing P_y , P_c and unstable load	55
Table 5.4	Ratios of Unstableload/ P_c , Unstableload/ P_y	80
Table 5.5	Overall behavior of cantilever beam	81

SYMBOLS AND ABBREVIATIONS

t	Thickness of rectangular cantilever beam cross section
h	Height of rectangular cantilever beam cross section
l	Length of rectangular cantilever beam
M_y	Yield moment for the rectangular cross-section
M_c	Plastic hinge moment
P_y	Force applied at the free-end of cantilever beam
P_c	Force applied at the free-end of cantilever beam when the fixed end is fully plastic
P_{eb}	Elastic buckling load applied at free end of rectangular cantilever beam
σ_y	Yield stress of the material
G	Shear modulus
E	Elastic modulus
ν	Poisson ratio
t'	Ratio of width by length of cantilever beam t/l
H	Ratio of height by width of cantilever beam h/t
$[D]$	Elasticity matrix
U	Strain energy
V	External work
$\{\epsilon\}$	Strain vector
$\{\sigma\}$	Stress vector
$\{u\}$	Nodal displacement vector
$[N]$	Matrix of shape functions.
$[K_e]$	Element stiffness matrix
$\{x\}$	Deformed vector
$\{X\}$	Unreformed vector
$[I]$	Identity matrix

CONTENTS

ABSTRACT	iii
ACKNOWLEDGEMENTS	iv
LIST OF FIGURES	v
LIST OF TABLES	vii
SYMBOLS AND ABBREVIATIONS	viii

1 INTRODUCTION

1.1 Finite Element Analysis of the Plastic Buckling of a Cantilever Beam	1
1.2 Objectives of the Thesis	3
1.3 Layout of the Thesis	3

2 BACKGROUND AND SCOPE OF WORK

2.1 Literature Review	5
2.1.1 Buckling Analysis	6
2.1.2 Finite Element Analysis on Plastic Behaviors	10
2.2 Scope of the Study	14
2.2.1 Material Nonlinearity	14
2.2.2 Geometric Nonlinearity	14
2.2.3 Solution Method	15
2.2.4 General Model for Buckling Analysis	15
2.2.5 Numerical Study on Plastic Buckling Analysis	16

3 FINITE ELEMENT FORMULATION FOR PLASTIC ANALYSIS

3.1 Structural Fundamentals	17
3.1.1 Stress-strain Relationships	17
3.1.2 Derivation of Structural Matrices	20
3.2 Geometric Nonlinearities	23
3.2.1 Large Strain	24
3.2.2 Large Deflection	25
3.3 Material Nonlinearities	26
3.3.1 Yield Criterion	26
3.3.2 Flow Rule	27
3.3.3 Hardening Rule	27
3.3.4 Plastic Strain Increment	28
3.4 Newton-Raphson Procedure	29
3.4.1 Overview	29
3.4.2 Convergence	33

4 IMPLEMENTING FINITE ELEMENT PLASTIC BUCKLING ANALYSIS

4.1 Introduction on ANSYS	34
4.2 Buckling Analysis	35
4.2.1 Nonlinear Buckling Analysis	35
4.2.2 Eigenvalue Buckling Analysis	36
4.3 Implementation the Plastic Buckling of Cantilever	37
4.3.1 Description of the Problem	37
4.3.2 Element Type	38
4.3.3 Material Properties	38
4.3.4 Solid Modeling and Boundary Conditions	39
4.3.5 Nonlinear Analysis	39
4.3.6 Deflection Results vs. Force Results	40

5 NUMEERICAL STUDIES AND DISCUSSIONS	
5.1 Numerical Applications	42
5.2 Investigation of Plastic Buckling Regime	43
5.2.1 Boundary of Elastic Buckling and Yield	43
5.2.2 Boundary of Plastic Buckling and Plastic Hinge Collapse	50
5.2.3 Procedure for Analysis of a Specific Case	51
5.3 Finite Element Analysis Results	54
5.3.1 ANSYS Results for Plastic Buckling and Plastic Hinge Boundary	54
5.2.2 Overall Behavior of Cantilever Beam	79
5.4 Discussions	82
6 CONCLUSIONS AND RECOMMENDATIONS	
6.1 Conclusions	83
6.2 Recommendations	84
REFERENCES	86
APPENDIX A	89
APPENDIX B	93
APPENDIX C	95

Chapter I

INTRODUCTION

1.1 Finite Element Analysis of the Plastic Buckling of a Cantilever Beam

Buckling analysis is one way to determine the critical load at which a structure becomes unstable. In plastic buckling, the structure experiences elastic deformation, yielding, partial plasticity, and collapse. If the structure becomes unstable before yielding, it is elastic buckling, which is well studied by previous researchers. When the instability lies in the partial yielding range, the structure fails by plastic buckling.

Finite element analysis is a numerical method for analysis of structures or other continua field. The method requires discretization of a given structure into a set of finite elements. A typical finite element analysis includes element type selection, geometric modeling, application of boundary condition, load application, system solution and post-processing.

For the plastic buckling analysis of structures, finite element analysis employs a nonlinear static plastic analysis with gradually increasing loads to seek the load level at which the structure becomes unstable. Nonlinear plastic finite element analysis requires treatment for both geometric and material nonlinearities. There are two kinds of geometric nonlinearities concerned in plastic buckling analysis, large strain and large deflection. Large strain assumes that the strains are no longer infinitesimal when structure's shape changes. Large deflection assumes that the rotations are large. Material nonlinearities are due to the nonlinear relationship between stress and strain. Elastic-perfectly plastic material nonlinearity is used in this work.

A finite element model of a rectangular cross section cantilever beam is presented. In this model, Young's modulus, Poisson ratio, and yielding stress are set as variables. All dimensions of the cantilever beam are also set as variables. The overall behavior is studied by both analytical and finite element analyses. Two non-dimensional parameters, the ratio of thickness to length t/l , and the ratio of depth to thickness h/t are used to evaluate the overall behavior of cantilever beam. The behavior of the beam can be classified into three types, elastic buckling, plastic buckling, and plastic collapse. These three behavior areas are separated by the boundary of elastic buckling and yielding, and boundary of plastic buckling and collapse.

1.2 Objectives of the Thesis

There is a need to develop general design guidelines to prevent plastic buckling in stiffened panels. This report addresses one aspect of this problem. Stiffened panels consist of stiffener frames and a thin shell. The stability of the stiffened panels is strongly influenced by the behavior of the stiffeners. Stiffeners can be simplified as beams. A full understanding of the stability properties of beams will help understand the stability properties of stiffened panels.

The approach used in this work is to develop a general finite element model for the buckling analysis which can be adapted to different dimensions of rectangular cantilever beams. The material of the beam is defined as elastic-perfectly plastic, which uses two parameters: Young's modulus and yield stress. The objective of this work is to study the overall behavior of rectangle cross section cantilever beams subjected to concentrated loads on the free-end. The overall behavior is defined as a "failure map" with boundaries for elastic buckling and yielding, plastic buckling and collapse.

1.3 Layout of the Thesis

Chapter one gives an introduction to the finite element method for plastic buckling analysis. Chapter two provides a detailed literature review of the relevant topics to plastic

buckling analysis for cantilever beam analysis and defines the scope of the study. The plastic buckling analysis methods along with the fundamental theory of structures, geometric and material nonlinearities, and the nonlinear solution method is given in chapter three. The implementation of the plastic buckling analysis by ANSYS is presented in chapter four. Chapter five shows a numerical study of the plastic buckling and collapse boundary for the plastic buckling of cantilever beams. The conclusions of the study and recommendations are included in chapter six.

Chapter II

BACKGROUND

AND SCOPE OF WORK

2.1 Literature Review

Buckling analysis of structures was studied initially by Euler [1] in his famous work on elastic analysis on the column. In it, he had provided an analytical solution to the stability problem. After that, there were extensive research [2] on various types of structure stability. These studies not only covered various structure types, but also have been dealt with different domain of material properties. The plastic instability has been studied by researchers [4-10] and various methods have been applied to this issue.

Finite element analysis for structural stability problems has been possible after methods[2] have been developed for the material and geometry nonlinearities. The finite element analysis method for buckling analysis has been treated as a nonlinear large deflection analysis of structures including geometric and material nonlinearity. Hence,

the nonlinear methods are crucial for the structural buckling and even postbuckling analysis.

First, different approaches to structural stability, especially for the cantilever beams will be reviewed; and then the various nonlinear finite element techniques applied to the plastic analysis will also be reviewed.

2.1.1 Buckling Analysis

Sritawat Kitipornchai and Nicholas S. Trahair [4] investigated the inelastic buckling of simply supported steel I-beams with central concentrated loads. They did this by adapting a basic theoretical model of the inelastic buckling of beams under uniform moment by modifying the differential equations, which govern the elastic buckling of tapered mono-symmetric I-beams. The resulting differential equations were solved for critical loads by using the method of finite integrals. A simple approximate model was also analyzed, in which the shear centerline was idealized by a series of discontinuous straight lines, parallel to the longitudinal axis. It was found that this approximate method gave solutions that were very close to the more accurate values. They also studied the effects of residual stresses, and found that these caused significant variations in the inelastic buckling strengths. The effects of the height of the point of application of the load and of the distribution of the major axis bending moment were investigated by comparing the values of the dimensionless critical moments for beams under uniform moment. This

comparison was made on the basis of a modified slenderness ratio, defined by the square root of yield moment divided by elastic buckling moment.

Mohamed H. El-Zanaty and David W. Murray [5] presented a general formulation for the elastic and plastic nonlinear analyses of steel structures. The plastic analysis includes the effects of residual stresses, strain hardening, gradual expansion of plasticity through the cross section and the spread of plastic zones along the member length. The technique is illustrated by solving a variety of problems for which alternative results are available. A geometrically nonlinear formulation for the analysis of steel frames was presented. The simple geometric approximation permits the virtual work equations to be derived in a manner consistent with the full nonlinear strain displacement equations without introducing further approximations. When this geometric nonlinear theory was combined with Shanley's tangent modulus concepts, and the incremental Newton-Raphson equations formed by the finite element method, a numerical technique emerges which is capable of solving plastic structural stability problems for arbitrary geometry.

Peter F. Dux and Sritawat Kitipornchai [6] introduced methods to obtain buckling loads of beams with a plastic moment gradient. A plastic parameter, the stiffness modification factor, is used to estimate equivalent uniform tangent modulus rigidities for partially yielded beams. From this they developed a buckling moment equation. For laterally continuous beams, a step-by-step procedure, which allows for interaction between adjacent segments is proposed. The structure is reduced to a critical assemblage of beam segments. The stiffness modification factor is used to quantify segment end interaction

and an effective length factor is found for the critical segment. The buckling moment equation is used to estimate the beam capacity. The results are comparable with theoretical and experimental results. The new method proposed in this paper extends the refined elastic analysis to plastic continuous beams. It incorporates a new equation for single span beams and includes several effective length charts. The method also introduces a more rigorous appraisal of the effects of yielding on segment interaction.

Mark A. Bradford, et al., [7] introduced an accurate line model based on the finite element method, for analyzing the plastic lateral buckling of I-section beams and beam-columns. The pre-buckling in plane bending is analyzed using a geometrically nonlinear finite element method that accounts for the effects of pre-buckling displacements and residual stresses on yielding. The results of the pre-buckling analysis allow the distributions of yielding and strain hardening throughout the beam to be determined. The out of plane flexural-torsional buckling of the inelastic beam is analyzed by adapting an elastic monosymmetric finite element. For this element, deflections and twists are referred to an arbitrary axis along the mid-height of the web, instead of along the shear center axis. The elastic element is adapted for plastic buckling and strain hardening. The method achieved accurate results, albeit with simple assumptions.

N. S. Trahair and S. Kitipornchai [8] studied the inelastic flexural-torsional buckling of simply supported I-beams under a uniform moment. Tangent modulus theory of buckling was applied to the basic theoretical model, which is simpler than reduced modulus theory and leads to conservative estimates of the critical moment. It was suggested that using the

strain-hardening modulus in the yielded regions of the beam is better than the reduced modulus, but that the critical moments are not greatly affected by assuming that the tangent modulus is zero, as had been done by previous investigators. They also studied the influence of residual stresses on the critical moments. It was found that the effect of this on the inelastic critical moment is quite significant. The effects of the magnitude and pattern of residual stresses on the critical moments have also been investigated. It was found that changes in the residual stress lead to variations in the yielded regions in the cross section, and consequent variations in the section rigidities. These variations cause very significant changes in the inelastic critical moments. As residual stresses can significantly change the inelastic critical moments and as residual stresses exist in all rolled steel sections, it was concluded that residual stresses should be accounted for.

James F. Doyle [9] presented a method to assemble an approximate stiffness matrix, and after applying boundary conditions, to determine the eigenvalues (buckling loads) of the structure. This method set up approximate load and displacement functions and then generated approximate global stiffness matrix, and solved the eigenvalue problem.

N. S. Trahair [10] has applied tangent modulus theory to inelastic buckling of beams. Compared to reduced modulus theory, the tangent modulus theory appeared to be invalid for inelastic materials. Nevertheless, experiments showed that it leads to more accurate predictions than the apparently rigorous reduced modulus theory. The reason is that when buckling deflections are accompanied by simultaneous increases in the applied load of sufficient magnitude to prevent strain reversal, all the stress and strain increments are

related by the tangent modulus, the buckling load is equal to the tangent modulus load. The application of the tangent modulus theory to the inelastic flexural-torsional buckling of a steel member requires appropriate values of the tangent shear modulus to be used when evaluating the contributions of the yielded and strain-hardened regions to the effective torsional rigidity. Before an inelastic out-of-plane buckling analysis can be made, the in-plane bending must be analyzed so that the distributions of the elastic, yielded, and strain-hardened regions throughout the member can be determined. The effective out-of-plane rigidity, which contributes to the inelastic buckling resistance, can be evaluated using these distributions. The energy method is then applied to get the equation for the buckling and generated the stiffness and stability matrices. In general, the computation procedure was to iterate through a series of load levels towards a solution. At each load level the in-plane analysis was performed, and the results were then used to establish the matrix and the value of its determinant was calculated until a zero value for the determinant is found, which defined a buckling load.

2.1.2 Finite Element Analysis on Plastic Behaviors

F. Brezzi [11] analyzed the behavior of a finite dimensional approximation of the Galerkin type in a neighborhood of a simple critical point. Error bounds of optimal type

are derived and some computational aspects are also treated. He presented some methods in the theory of approximation of nonlinear problems, with a particular attention to the behavior of the approximate solutions in a neighborhood of singular points, such as normal limit points and bifurcation points. Although some computational aspects are briefly sketched, the main interest focused on the problem of error bounds. The well-known definitions of the singularities were given, for simplicity, in finite dimension. It also presented the continuous problem and the abstract hypotheses on the finite dimensional approximation method on the error estimate.

C. S. Desai and H. V. Phan [12] developed a finite element procedure for stress deformation analysis of three-dimensional solid bodies including geometric and material nonlinearities. The formulation is applicable to general three-dimensional problems. It allows for consistent definitions of stress, stress rate and constitutive laws and uses the original Newton-Raphson technique for incremental iterative analysis. Six different constitutive laws based on von Mises, Mohr-Coulomb, Drucker-Prager, critical state, capped and viscoplastic criteria are incorporated in the formulation and the computer code. They can be used depending upon the material property involved in a given problem. It provided a viable formulation and computational scheme for solution of three-dimensional solid bodies including geometric and material nonlinearities, and it is particularly useful for large plastic strains.

Y. Yamada, T. Hirakwa A. S. Wifi [13] established a rational unified approach to finite strain problems combined with material nonlinearities. The geometric stiffness and load

correction matrices in large deformation problems are discussed, and emphasis is placed on the treatment of the boundary conditions where coupling exists in the stresses. The formulation is applicable to plastic instability analysis. Proper choice of stress rate is essential in the formulation of large strain analysis, as is the spin of principal stress axes rather than that of the element. The method for the plastic work covered only the earlier stages of deformation, far from the steady state. The authors extended the work to similar types of steady state large deformation problems.

E. Riks [14] presented a numerical solution of systems of equations of discrete variables, which represent the nonlinear behavior of elastic systems under conservative loading conditions. In particular, an incremental approach to the solution of buckling and snap-through problems is explored. The numerical solution for covered several systems: the computation of nonlinear equilibrium paths with continuation through limit points and bifurcation points; the determination of critical equilibrium states. Characteristic to the procedures employed is the use of the length of the equilibrium path as a control parameter. This feature, together with the second order iteration method of Newton, offers a reliable basis for the procedures described.

S. L. Chan [15] presents a numerical procedure for accurate determination of a limit or a bifurcation point. The method minimizes simultaneously the first and the second variations of an admissible functional or iterates to satisfy the equilibrium and the semi-definite condition for the tangent stiffness matrix. Using the technique, the critical load and its conjugated displacement can be computed explicitly and accurately in an analysis, leading to a more exact prediction of the critical load of a structure. It demands an

additional load cycle which normally requires more number of iterations than other methods because of the need to satisfy not only the equilibrium condition to determine the critical point, and requires the semi-definite tangent stiffness matrix. This computation effort is however, minimal when compared to the approach of tracing the load versus deflection path by using a small load step size to narrow the loading range within which the critical load occurs. The numerical method can be easily incorporated into a computer program for non-linear finite element analysis and enhanced the user-friendliness and accuracy of the program.

Chen [16] also introduced the Minimum Residual Displacement Method, which is used together with the concept of the effective tangent stiffness matrix for braced members. He presented a geometric and material non-linear analysis procedure for structures, using a solution algorithm of minimizing the residual displacements. This new non-linear solution technique is optimized in the Newton-Raphson scheme since it follows the shortest path to achieve convergence. It introduced the concept of the effective tangent stiffness matrix, which is found to be efficient, simple and logical in handling the non-linear analysis of frames with braced members and in separating multiple bifurcation points. The technique is capable of handling geometric and /or material non-linear problems exhibiting snap-through, softening and stiffening behavior.

2.2 Scope of the Study

Finite element plastic buckling analysis is a nonlinear static analysis extended to a point where the structure reaches its limit load or maximum load. The basic approach in a

nonlinear plastic buckling analysis is to constantly increment the applied loads until the solution begins to diverge. Nonlinearities such as material plasticity and geometric nonlinearity are included in the analysis. Iterative incremental solution procedure for the nonlinear equations is applied to solve the nonlinear problem.

2.2.1 Material Nonlinearity

Most common engineering materials exhibit a linear stress-strain relationship up to a stress level known as the proportional limit. Beyond this limit, the stress-strain relationship will become nonlinear. Material nonlinearities are due to the nonlinear relationship between stress and strain, that is, the stress is a nonlinear function of the strain. Nonlinear stress-strain relationships are a common cause of nonlinear structural behavior. The material non-linearity is implemented in the finite element method. Material models for nonlinearities include multilinear plasticity and elastic-perfect plasticity. For this work, the elastic-perfectly plastic material non-linearity is employed.

2.2.2 Geometric Nonlinearity

Geometric nonlinearities refer to the nonlinearities that are due to the changing geometry as it deflects. There are two types of geometric nonlinearities concerned in this work: large strain and large deflection. Large strain analysis accounts for strains in an element when they are no longer small. This changes an element's shape and orientation and hence affect the stiffness of the element. Large deflection assumes that the rotations are

large while the strains may still be small. If a structure experiences large deformations, its changing geometric configuration can cause the structure to respond nonlinearly.

2.2.3 Solution Method

When the finite element model is set up for nonlinear analysis including material and geometric nonlinearities, an appropriate nonlinear solution method should be applied. The Newton-Raphson technique is an iterative incremental method to achieve convergence. The load is divided into several substeps, applied by the Newton-Raphson method to get convergence.

2.2.4 General Model for Buckling Analysis

The general models for plastic buckling analysis are developed in this thesis for the study of variable dimension rectangle cross section cantilever beams subjected to a concentrated load at the free-end. The model includes material nonlinearity, which in this work is elastic perfectly plastic defined by the Young's modulus and yielding stress. These two parameters are variable. The dimensions of the cross section are also changeable for the different configurations.

2.2.5 Numerical Study on Plastic Buckling Analysis

In this work a numerical study of cantilever beams along with the analytical solution of the elastic buckling, yielding and collapse of cantilever beam are given. Uniform non-dimensional parameters are set up as criteria for the overall behavior. The overall

behavior of the rectangle cross section cantilever beam is separated to three regions by the boundary of elastic buckling and yielding, and plastic buckling and plastic hinge collapse.

Chapter III

FINITE ELEMENT FORMULATION FOR PLASTIC ANALYSIS

The finite element analysis of plastic buckling is a plastic static solution process reaching the unstable point. Formulation for plastic buckling includes structural fundamentals, geometric nonlinearity, material nonlinearity, and Newton-Raphson method.

3.1 Structural Fundamentals

3.1.1 Stress-Strain Relationships

The linear material stresses are related to strains [17][32] by

$$\{\sigma\} = [D]\{(\varepsilon) - \{\varepsilon^0\}\} \quad 3.1$$

Where $\{\sigma\}$ = stress vector = $[\sigma_x \quad \sigma_y \quad \sigma_z \quad \sigma_{xy} \quad \sigma_{yz} \quad \sigma_{zx}]^T$

$[D]$ = elasticity matrix

$$\{\varepsilon\} = \text{strain vector} = [\varepsilon_x \quad \varepsilon_y \quad \varepsilon_z \quad \varepsilon_{xy} \quad \varepsilon_{yz} \quad \varepsilon_{zx}]^T$$

$$\{\varepsilon^{th}\} = \text{thermal strain vector}$$

The stress vector is shown in Figure 3.1. The sign convention for direct stresses and strains used is that tension is positive and compressions negative. For the shears, positive is when two applicable positive axes point toward each other. Shear strains are engineering shear strains, not tensor shear strains.

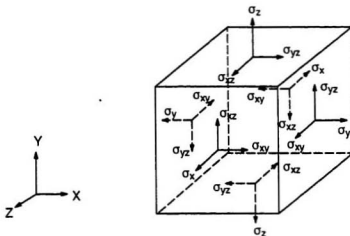


Figure 3.1 Stress vector definition

Equation 3.1 may also be inverted to

$$\{\varepsilon\} = \{\varepsilon^{th}\} + [D]^{-1} \{\sigma\} \quad 3.2$$

For 3-D case, the thermal strain vector is

$$\{\varepsilon^{th}\} = \Delta T [\alpha_x \quad \alpha_y \quad \alpha_z \quad 0 \quad 0 \quad 0]^T \quad 3.3$$

where α_x = thermal coefficient of expansion in the x direction

$$\Delta T = T - T_{REF}$$

T = current temperature at the point in question

T_{REF} = reference (strain-free) temperature

Expanding Equation 3.2 with Equation 3.3 and writing out the six equations explicitly,

$$\varepsilon_x = \alpha_x \Delta T + \frac{\sigma_x}{E_x} - \frac{\nu_{xy} \sigma_y}{E_y} - \frac{\nu_{xz} \sigma_z}{E_z} \quad 3.4$$

$$\varepsilon_y = \alpha_y \Delta T - \frac{\nu_{yx} \sigma_x}{E_x} + \frac{\sigma_y}{E_y} - \frac{\nu_{yz} \sigma_z}{E_z} \quad 3.5$$

$$\varepsilon_z = \alpha_z \Delta T - \frac{\nu_{zx} \sigma_x}{E_x} - \frac{\nu_{zy} \sigma_y}{E_y} + \frac{\sigma_z}{E_z} \quad 3.6$$

$$\varepsilon_{xy} = \frac{\sigma_{xy}}{G_{xy}} \quad 3.7$$

$$\varepsilon_{xz} = \frac{\sigma_{xz}}{G_{xz}} \quad 3.8$$

$$\varepsilon_{yz} = \frac{\sigma_{yz}}{G_{yz}} \quad 3.9$$

Where typical terms are

ε_x = direct strain in the x direction

ε_{xy} = shear strain in the x-y plane

σ_x = direct stress in the x direction

σ_{xy} = shear stress on the x-y plane

E_x = Young's modulus in the x direction

ν_{xy} = Poisson's ratio relating ϵ_x to σ_x/E_y

$\bar{\nu}_{xy}$ = Poisson's ratio relating ϵ_x to σ_y/E_x

3.1.2 Derivation of Structural Matrices

The principle of virtual work [28] states that a very small virtual change of the internal strain energy must be offset by an identical change in external work due to the applied loads,

$$\delta U = \delta V \quad 3.10$$

where U = strain energy = $U_1 + U_2$

V = external work = $V_1 + V_2$

δ = virtual operator

The virtual strain energy is

$$\delta U_1 = \int_{vol} \{\delta \epsilon\}^T \{\sigma\} d(vol) \quad 3.11$$

where $\{\epsilon\}$ = strain vector

$\{\sigma\}$ = stress vector

vol = volume of element

Continuing the derivation assuming linear materials and geometry, Equation 3.1 and 3.11 are combined to give

$$\delta U_1 = \int_{vol} (\{\delta \epsilon\}^T [D] \{\epsilon\} - \{\delta \epsilon\}^T [D] \{\epsilon^{th}\}) d(vol) \quad 3.12$$

The strains may be related to the nodal displacement by

$$\{\varepsilon\} = [B]\{u\} \quad 3.13$$

where $[B]$ = strain-displacement matrix, based on the element shape functions

$$\{u\} = \text{nodal displacement vector}$$

It will be assumed that all effects are in the global Cartesian system. Combining Equation 3.13 with Equation 3.12, and noting that $\{u\}$ does not vary over the volume

$$\delta U_1 = \{\delta u\}^T \int_{vol} [B]^T [D] [B] d(vol) \{u\} - \{\delta u\}^T \int_{vol} [B]^T [D] \{\varepsilon^0\} d(vol) \quad 3.14$$

Another form of virtual strain energy is when a surface moves against a distributed resistance, as in a foundation stiffness. This may be written as

$$\delta U_2 = \int_{area} \{\delta w_n\}^T \{\sigma\} d(area) \quad 3.15$$

where $\{w_n\}$ = motion normal to the surface

$\{\sigma\}$ = stress carried by the surface

$area$ = area of the distributed resistance

Both $\{w_n\}$ and $\{\sigma\}$ will usually have only one non-zero component. The point-wise normal displacement is related to the nodal displacements by

$$\{w_n\} = [N_n] \{u\} \quad 3.16$$

Where $[N_n]$ = matrix of shape function for normal motions at the surface

The stress $\{\sigma\}$ is

$$\{\sigma\} = k \{w_n\} \quad 3.17$$

where k = the foundation stiffness in units of force per length per unit area

Combining Equations 3.15 through 3.17, and assuming that k is constant over the area

$$\delta U_2 = \{\delta u\}^T k \int_{area_e} [N_n]^T [N_n] d(area_e) \{u\} \quad 3.18$$

Next, the external virtual work will be considered.

The displacement within the element are related to the nodal displacements by

$$\{w\} = [N] \{u\} \quad 3.19$$

where $[N]$ = matrix of shape functions.

Nodal forces applied to the element can be accounted for by

$$\delta V_1 = \{\delta u\}^T \{F_e^{nd}\} \quad 3.20$$

Where $\{F_e^{nd}\}$ = nodal forces applied to the element

The pressure force vector formulation starts with

$$\delta V_2 = \int_{area_p} \{\delta w_n\}^T \{P\} d(area_p) \quad 3.21$$

where $\{P\}$ = the applied pressure vector (normally contains only one non-zero component)

$area_p$ = area over which pressure acts

Combining Equations 3.19 and 3.21

$$\delta V_2 = \{\delta u\}^T \int_{area_p} [N_n]^T \{P\} d(area_p) \quad 3.30$$

All material properties for stress analysis elements are evaluated at the average temperature of each element. Finally, Equations 3.10, 3.14, 3.18, 3.20 and 3.22 may be combined to give

$$\begin{aligned} & \{\delta u\}^T \int_{vol} [B]^T [D] [B] d(vol) \{u\} - \{\delta u\}^T \int_{vol} [B]^T [D] \{\epsilon^{th}\} d(vol) \\ & + \{\delta u\}^T k \int_{area_e} [N_n]^T [N_n] d(area_e) \{u\} \end{aligned}$$

$$= \{\delta u\}^T \int_{\text{area}_e} [N_n]^T \{P\} d(\text{area}_e) + \{\delta u\}^T \{F_e^{\text{nd}}\} \quad 3.23$$

Noting that the $\{\delta u\}^T$ vector is a set of arbitrary virtual displacements common in all of the above terms, the condition required satisfy Equation 3.31 reduces to

$$([K_e] + [K_e'])\{u\} - \{F_e^{\text{th}}\} = \{F_e^{\text{pr}}\} + \{F_e^{\text{nd}}\} \quad 3.24$$

Where $[K_e] = \int_{\text{vol}} [B]^T [D][B] d(\text{vol})$ = element stiffness matrix

$[K_e'] = k \int_{\text{area}_e} [N_n]^T [N_n] d(\text{area}_e)$ = element foundation stiffness matrix

$\{F_e^{\text{th}}\} = \int_{\text{vol}} [B]^T [D]\{\epsilon^{\text{th}}\} d(\text{vol})$ = element thermal load vector

$\{F_e^{\text{pr}}\} = \int_{\text{area}_e} [N_n]^T \{P\} d(\text{area}_e)$ = element pressure vector

Equation 3.24 represents the equilibrium equation on one element basis.

3.2 Geometric Nonlinearities

For our problem interests, there are two types of geometric nonlinearities [18][19] should be considered: Large strain assumes that the strains are no longer infinitesimal (they are finite). Shape changes (e.g. area, thickness, etc.) are also accounted for. Rotation may also be large; Large deflection assumes that the rotations are large but the mechanical strains (those that cause stresses) are small. The structure is assumed not to change shape except for rigid body motions.

3.2.1 Large Strain

When the strains in a material exceed more than a few percent, the changing geometry due to this deformation can no longer be neglected. Analyses including this effect are called large strain, or finite strain, analyses. The theory of large strain computations can be addressed by defining a few basic physical quantities (motion and deformation) and the corresponding mathematical relationship. The applied loads acting on a body make it move from one position to another. This motion can be defined by studying a position vector in the "undeformed" and "undeformed" configuration. Say the position vectors in the "undeformed" and "undeformed" state are represented by $\{x\}$ and $\{X\}$ respectively, then the motion (displacement) vector $\{u\}$ is computed by Figure 3.2

$$\{u\} = \{x\} - \{X\} \quad 3.25$$

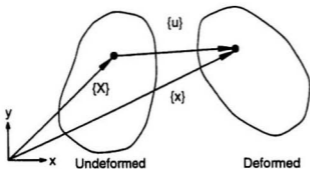


Figure 3.2 Position vectors and motion of a deforming body

The deformation gradient is defined as

$$[F] = \frac{\partial \{x\}}{\partial \{x_0\}} \quad 3.26$$

Which can be written in terms of the displacement of the point by Equation 3.25 as

$$[F] = [I] + \frac{\partial \{u\}}{\partial \{x_0\}} \quad 3.27$$

where $[I]$ = identity matrix

The information contained in the deformation gradient $[F]$ includes the volume change, the rotation and the shape change of the deforming body. The volume change at a point is

$$\frac{dV}{dV_0} = \det[F] \quad 3.28$$

where V_0 = original volume

V = current volume

$\det[\bullet]$ = determinant of the matrix

The deformation gradient can be separated into a rotational and a shape change using the right polar decomposition theorem

$$[F] = [R][U] \quad 3.29$$

where $[R]$ = rotation matrix ($[R]^T [R] = [I]$)

$[U]$ = right stretch (shape change) matrix

3.2.2 Large Deflections

If the rotations are large but the mechanical strains are small, then a large deflection procedure can be used. A large deflection analysis is performed in a static analysis when the appropriate element type is used. Large deflection theory follows a similar

development of large strain, except that the logarithmic strain measure is replaced by small strain measure

$$[\varepsilon] = [U] - [I] \quad 3.30$$

where $[U]$ = stretch matrix

$[I]$ = 3 x 3 identity matrix

3.3 Material Nonlinearities

Material nonlinearities [19] are due to the nonlinear relationship between stress and strain, that is the stress is a nonlinear function of the strain. The thesis focuses on the rate-independent plasticity, which is characterized by the irreversible instantaneous straining that occurs in a material once a certain level of stress is reached. The plastic strains are assumed to develop instantaneously, that is, independent of time. Plasticity theory provides a mathematical relationship that characterizes the elasto-plastic response of materials. There are three ingredients in the rate-independent plasticity: the yield criterion, flow rule and the hardening rule

3.3.1 Yield Criterion

The yield criterion determines the stress level at which yielding is initiated. For multi-component stresses, this is represented as a function of the individual components,

$f(\{\sigma\})$, which can be interpreted as an equivalent stress σ_e :

$$\sigma_e = f(\{\sigma\}) \quad 3.31$$

where $\{\sigma\}$ = stress vector

When the equivalent stress is equal to a material yield parameter σ_y ,

$$\sigma_e = f(\{\sigma\}) \quad 3.32$$

the material will develop plastic strains. If σ_e is less than σ_y , the material is elastic and the stress will develop according to the elastic stress-strain relations. Note that the equivalent stress can never exceed the material yield since in this case plastic strains would develop, thereby reducing the stress to the material yield.

3.3.2 Flow Rule

The flow rule determines that direction of plastic straining and is given as:

$$\{d\epsilon^p\} = \lambda \left\{ \frac{\partial Q}{\partial \sigma} \right\} \quad 3.33$$

where

λ = plastic multiplier (which determines the amount of plastic straining)

Q = function of stress termed the plastic potential (which determines the direction of plastic straining)

If Q is the yield function (as normally assumed), the flow rule is termed associative and the plastic strains occur in a direction normal to the yield surface.

3.3.3 Hardening Rule

The hardening rule describes the changing of the yield surface with progressive yielding, so that stress states for subsequent yielding can be established. Two hardening rules are available: isotropic work hardening and kinematic hardening. In isotropic work

hardening, the yield surface remains centered about its initial centerline and expands in size as the plastic strains develop. For materials with isotropic plastic behavior this is termed isotropic hardening. Kinematic hardening assumes that the yield surface remains constant in size and the surface translates in stress space with progressive yielding.

3.3.4 Plastic Strain Increment

If the equivalent stress computed using elastic properties exceeds the material yield, then plastic straining must occur. Plastic strains reduce the stress states so that it satisfies the yield criterion, Equation 3.32. Based on the theory presented in the previous, the plastic strain increment is readily calculated. The hardening rule states that the yield criterion changes with isotropic work hardening and/or with kinematic hardening. Incorporating these dependencies into Equation 3.32 gives

$$F(\{\sigma\}, \aleph, \{\alpha\}) = 0 \quad 3.34$$

where \aleph = plastic work

$\{\alpha\}$ translation of yield surface

\aleph and $\{\alpha\}$ are termed internal or state variables.

Specifically, the plastic work is the sum of the plastic work done over the history of loading:

$$\aleph = \int \{\sigma\}^T \{d\epsilon^p\} \quad 3.35$$

and translation of the yield surface is also history dependent and is given as:

$$\{\alpha\} = \int C \{d\epsilon^p\} \quad 3.36$$

where C is a material parameter. $\{\alpha\}$ represents the location of the center of the yield surface and moves in the direction of plastic straining.

3.4 Newton-Raphson Procedure

3.4.1 Overview

The finite element discretization process yields a set of simultaneous equations

$$[K]\{u\} = \{F^a\} \quad 3.37$$

where

$[K]$ = coefficient matrix

$\{u\}$ = vector of unknown DOF (degree of freedom) values

$\{F^a\}$ = vector of applied loads

If the coefficient matrix $[K]$ is itself a function of the unknown DOF values or their derivatives then Equation 3.37 is a nonlinear equation. The Newton-Raphson method [21][22][32] is an iterative process of solving the nonlinear equations and can be written as

$$[K_r^T]\{\Delta u_i\} = \{F^a\} - \{F_i^{nr}\} \quad 3.38$$

$$\{u_{i+1}\} = \{u_i\} + \{\Delta u_i\} \quad 3.39$$

where

$[K_r^T]$ = Jacobian matrix

$\{F_i^{nr}\}$ = vector of restoring loads corresponding to element internal loads

i = subscript representing the current equilibrium iteration

Both $[K_i^T]$ and $\{F_i^m\}$ are evaluated based on the values given by $\{u_i\}$. The right-hand side of Equation 3.38 is the residual or out-of-balance load vector, i.e., the amount the system is out of equilibrium. One single solution iteration is depicted graphically in Figure 3.3 for a one DOF model. In a structural analysis, $[K_i^T]$ is the tangent stiffness matrix, $\{u_i\}$ is the temperature vector and $\{F_i^m\}$ is the restoring force vector calculated from the element stresses. As seen in Figure 3.3, more than one Newton-Raphson iteration is needed to obtain a converged solution.

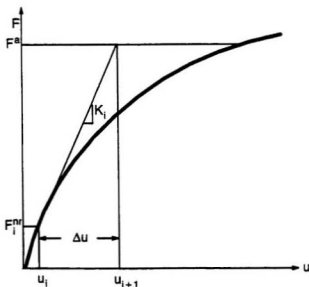


Figure 3.3 Newton-Raphson solution - one iteration

Figure 3.4 shows the solution of the next iteration ($i+1$) of the example from Figure 3.3. The subsequent iterations would proceed in a similar manner. The solution obtained at

the end of the iteration process would correspond to load level $\{F^a\}$. The final converged solution would be in equilibrium, such that the restoring load vector $\{F_r^m\}$ would equal the applied load vector $\{F^a\}$ or at least to within some tolerance. None of the intermediate solutions would be in equilibrium.

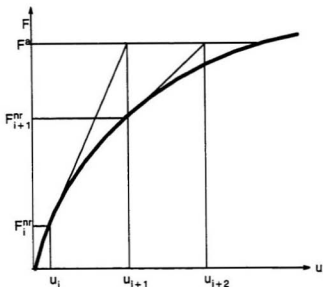


Figure 3.4 Newton -Raphson solution - next iteration

If the analysis included path-dependent nonlinearities such as plasticity, then the solution process requires that some intermediate steps be in equilibrium in order to correctly follow the load path. This is accomplished effectively by a step-by-step incremental analysis; i.e., the final load vector $\{F^a\}$ is reached by applying the load in increments and performing the Newton-Raphson iterations at each step

$$[K_{n,j}^T] \{\Delta u_i\} = \{F_n^a\} - \{F_{n,j}^{nr}\}$$

3.40

where

$[K_{n,j}^T]$ = tangent matrix for time step n, iteration I

$\{F_{n,j}^{nr}\}$ = restoring force vector for time step n, iteration I

$\{F_n^a\}$ = total applied force vector at time step n

This process is the incremental Newton-Raphson procedure and is shown in Figure 3.5.

The Newton-Raphson procedure guarantees convergence if and only if the solution at any iteration $\{u_i\}$ is "near" the exact solution.

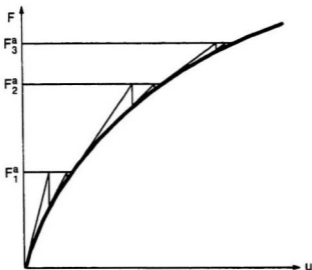


Figure 3.5 Incremental Newton-Raphson procedure

3.4.2 Convergence

The iteration process described in the previous continues until convergence is achieved.

Convergence is assumed when

$$\|\{R\}\| < \varepsilon_R R_{ref} \quad (\text{out-of-balance convergence}) \quad 3.41$$

and/or

$$\|\{\Delta u_i\}\| < \varepsilon_u u_{ref} \quad (\text{DOF increment convergence}) \quad 3.42$$

where $\{R\}$ is the residual vector

$$\{R\} = \{F^o\} - \{F^{nr}\} \quad 3.43$$

which is the right-hand side of the Newton-Raphson Equation 3.38. $\{\Delta u_i\}$ is the DOF increment vector, ε_R and ε_u are the tolerances and R_{ref} and u_{ref} are reference values. $\|\bullet\|$ is a vector norm; that is, a scalar measure of the magnitude of the vector. Convergence, therefore, is obtained when the size of the residual disequilibrium is less than a tolerance times a reference value and /or when the size of the DOF increment is less than a tolerance times a reference value.

Chapter IV

IMPLEMENTING FINITE ELEMENT PLASTIC BUCKLING ANALYSIS

4.1 Introduction to ANSYS

The ANSYS program was introduced by Dr. John Swanson and Swanson Analysis System, Incorporated (SASI), in 1970. Since that time, the program has been developed to provide the finite element analysis and design technology to engineers. ANSYS is one of the most widely used and well established finite element analysis programs in the world.

The ANSYS program has capability to implement structural analysis. In addition to its extremely strong ability to set up complicated three-dimensional solid models, it can provide static and dynamic, elastic and plastic analysis on these three-dimensional

structures. ANSYS also has excellent pre and post processor capabilities, providing a friendly graphical user interface.

4.2 Buckling Analysis

Buckling analysis is a technique used to determine buckling loads, critical loads at which a structure become unstable, and buckling mode shapes, the characteristic shape associated with a structure's buckling response [29]. Two techniques are available in the ANSYS program for predicting the buckling load and buckling mode shape of a structure: nonlinear buckling analysis, and eigenvalue (or linear) buckling analysis.

4.2.1 Nonlinear Buckling Analysis

Nonlinear buckling analysis is simply a nonlinear static analysis extended to a point where the structure reaches its limit load or maximum load as depicted in Figure 4.1(a). Using the nonlinear technique, the model can include features such as initial imperfections, plastic behavior, gaps, and large deflection response. In addition, using deflection controlled loading, the model can even track the post buckling performance of the structure. The basic approach in a nonlinear buckling analysis is to constantly increment the applied loads until the solution begins to diverge. Be sure to use a sufficiently fine load increment as your loads approach the expected critical buckling load. It is important to recognize that an unconverged solution need not necessarily mean that the structure has reached its maximum load. It could also be caused by numerical instability, which might be corrected by refining the modeling technique. Tracking the load deflection history of the structure's response can help you decide whether an

unconverged load step represents actual structural buckling, or whether it reflects some other problems. Nonlinear buckling analysis is usually the more accurate approach compared to eigenvalue buckling analysis and is therefore recommended for design or evaluation of actual structures.

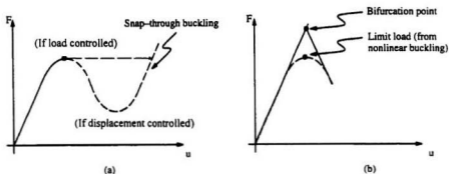


Figure 4.1 Buckling analysis: (a) Nonlinear load-deflection curve, (b) Comparing Linear (Eigenvalue) and nonlinear buckling curve

4.2.2 Eigenvalue Buckling Analysis

Eigenvalue buckling analysis predicts the theoretical buckling strength (the bifurcation point) of an ideal linear elastic structure. (See Figure 4.1(b)) This method corresponds to classical approach to elastic buckling analysis such as eigenvalue buckling analysis of an Euler column. However, imperfections and nonlinearities prevent most real world

structures from achieving their theoretical elastic buckling strength. Thus, eigenvalue buckling analysis often yields unconservative results. It should be decided if eigenvalue buckling analysis is appropriate for your application. The procedure consists of three main steps: constructing the model, obtaining the static solution to get structure stiffness matrix, obtaining the eigenvalue buckling solution.

4.3 Implementation the Plastic Buckling Analysis of a Cantilever Beam

4.3.1 Description of the Problem

When a cantilever beam is subjected to an external displacement or force on the free end, the initial behavior is elastic. The beam may buckle elastically. As the load/displacement increases, the fixed end of beam partially yields. After initial yield the beam will either buckle plastically or continue to yield until collapse. The behavior depending on the dimensions of the cantilever beam and the material properties. The behavior in the plastic regime is of interest because even if the structures are designed in the material elastic region, overloading can be happen for extraordinary load conditions. Further more, the plastic design may be much more economical for the industrial practice. Hence, clearly understanding the structure's overall behavior, especially in the plastic regime is essential for design practice.

In order to initiate buckling analysis, the applied force or displacement will be offset slightly from the center point. This breaks the perfect symmetry and allows buckling to occur. Otherwise the model would only exhibit plastic hinge collapse at the fixed end.

4.3.2 Element Type

The cantilever beam is set up as a three-dimensional model with plastic behavior. The buckling behavior requires an element with nonlinear capabilities for large strain and large displacement, while the material nonlinearity also is introduced in the element.

To fulfill the basic requirement, element SOLID 45 is chosen [32]. Solid 45 is used for the three-dimensional modeling of solid structure. The element is defined by eight nodes having three degrees of freedom at each node translations in the nodal x, y and z directions. The element has plasticity, creep, swelling, stress stiffening, large deflection, and large strain capabilities.

4.3.3 Material Properties

Material properties are required for the plastic analysis. In the model, the material is isotropic and elastic-perfectly plastic. Other types of plasticity also can be defined. Those types of plasticity include multilinear kinematic hardening, bilinear kinematic hardening etc. To properly define elastic perfectly plastic material behavior, the yield stress and young modulus is set, and the temperature is set to zero thus excluding temperature effects.

Several options are available in ANSYS to describe the plastic behavior. The Multilinear Isotropic Hardening (MISO) option was used to model the bilinear elastic-perfectly plastic. The MISO option uses the Von Mises criteria coupled with an isotropic work hardening assumption. Von Mises yield criterion and the Von Mises equivalent stress plots have been used because this type of plot provides the best way of assessing the behavior of the structural elements against the plastic hinge development.

4.3.4 Solid Modeling and Boundary Conditions

The advantage of solid modeling is that it can set up a parametric three-dimensional model very quickly. It is also very easy to modify the model. The model is set up with variables instead of directly defining every node of every element.

There are two types of boundary conditions applied to the structure. The displacement constraint is relatively simple, consisting of fixing three translations and three rotational freedom; while the force boundary condition includes the body force, surface pressure and external force applied on the model.

4.3.5 Nonlinear Analysis

The solution techniques employed essentially consists of solving simultaneous linear equilibrium equations which are successively updated to reflect changes in the material

and geometric stiffness as the structure is strained and distorts under increasing load. The incremental approach is driven by the load, which is incremented with each load step. Equilibrium at each load step is attained using a modified Newton-Raphson technique. ANSYS contains several features, which allow the user to control the solution process and these were used to good effect.

Using the correct load step increment is essential in a nonlinear analysis to attain a stable solution. This is especially true in regions where a rapid change in stiffness occurs. Such regions in the analysis were anticipated to be at first yield, at complete or partial yielding of the fixed end and then buckling or collapse for the whole cantilever beam. It is not possible, of course, to estimate with any degree of accuracy the load levels at which these events will occur hence the need for this study. The automatic time stepping feature in ANSYS was used to determine the load step increment. Based on the user specified initial, maximum and minimum load step increments, the program determines the appropriate load step increment based on the trend in convergence. If the rate of solution convergence increases, the load steps are increased, and vice versa.

4.3.6 Deflection Results vs. Force Results

Two options are available when user applies the load to the cantilever beam. At the center of free end, force or displacement may be applied. Consequently, the result will be deflection versus force, or force versus deflection. For the nonlinear plastic analysis, applying force may be suitable for the bifurcation instability process to predicate the

critical buckling point; whereas applying displacement is a more general analysis procedure, which can even reveal the post buckling behavior.

In stability experiments, the load is normally applied by a controlled displacement rather than a specified force. Force versus deflection graphical results will be employed to implement the plastic buckling analysis by ANSYS.

The Force versus deflection graphical results illustrate the overall beam behavior for specific dimensions of the beam at interesting critical points. The vertical and horizontal deflection curve and the force versus vertical deflection on some point of free end are used to determine the instability behavior of the structure, either plastic buckling or collapse. Stress results illustrate the stress components (stresses in x, y, z directions) or equivalent stress distribution of the whole structure.

The above is typical procedure for nonlinear plastic analysis for cantilever beam. If the solid model is adapted to other specific structures such as stiffened panel, frame and the material properties would be redefined. The aforementioned method is a general approach to determine the structure plastic behavior.

Chapter V

NUMERICAL STUDIES AND DISCUSSIONS

5.1 Numerical applications

Structures will experience different structural behaviors, depending on the material properties, the structural dimensions, the boundary conditions and the load pattern. Cantilever beams, when subjected to a concentrated force or displacement at the free end, deform until they reach an unstable point. The unstable point either will be plastic collapse caused by plastic hinge formation, or will be collapse because the structure reaches a point of instability. There are two cases of instability. First is the elastic buckling, in which all structure becomes unstable while still in the elastic region. The stresses in the structure are still less than the yield stress. Another case is plastic buckling,

in which some part of the structure experienced plastic stress while the rest of the structure is still in the elastic region.

The plastic buckling behavior of the cantilever beam is numerically studied in this thesis by nonlinear plastic buckling finite element analysis. In addition to the material properties, the dimensions of the cantilever beam will determine the structural behaviors. Dimensions vary from one beam to another, and different unstable behaviors will be presented. Through the detailed study of the different unstable cases, the thesis seeks the non-dimensional criteria to determine the structural plastic buckling behavior.

5.2 Investigation of Plastic Buckling Regime

5.2.1 Boundary of elastic buckling and yield

A cantilever beam will experience different structure behaviors due to the configuration of the cantilever's dimensions and the material properties. Dimensions of the cantilever beam are shown in the Figure 5.1. The load is a central force applied on the free end of the cantilever beam. It is presumed that the cantilever beam stays stable when the load is increased. There two critical loads, which we are interested in, the load P_y , the load when the top and bottom of beam's fixed end yield and P_c the load when the beam's fixed end section becomes fully plastic.

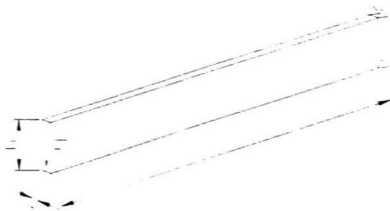


Figure 5.1 Cantilever beam subjected to concentrated load

From basic solid mechanics [23], we have

$$M_y = \sigma_y \frac{th^2}{6} \quad 5.1$$

M_y , Yield moment for the rectangular cross-section

σ_y , Yield stress of the material

We also have

$$M_y = P_y l \quad 5.2$$

from Equation 5.1 and 5.2 we have

$$P_y = \sigma_y \frac{th^2}{6l} \quad 5.3$$

When the fixed end of cantilever beam becomes fully plastic we have

$$M_p = \sigma_c \frac{th^2}{4} \quad 5.4$$

M_p moment when the fixed end is fully plastic(plastic hinge moment)

$$M_p = P_c l \quad 5.5$$

From Equation 5.4 and 5.5 we have

$$P_c = \sigma_c \frac{th^2}{4l} \quad 5.6$$

P_c and P_c provide lower and upper load boundaries plastic buckling.

In order to set up schematically plastic buckling finite element analysis results that are comparable to elastic buckling analysis results, non-dimensional parameters should be used to evaluate the structural behavior.

In order to find the critical non-dimensional parameters, let us first compare analytical results for the elastic buckling of rectangular cantilever beam subject to load at the free end.

The analytical elastic lateral-torsional buckling load for a single transverse load applied at the free end of a cantilever beam [26] is:

$$P_{eb} = \frac{0.669th^3}{l^2} \sqrt{\left(1 - 0.63 \frac{t}{h}\right) EG} \quad 5.7$$

$$G = \frac{E}{2(1 + \nu)}$$

P_{cb} elastic buckling load applied at the center of free end of rectangular cross-section cantilever beam

G = shear modulus

E = elastic modulus

ν = Poisson ratio

Recognize that the ratio of $\frac{t}{l}$ and the ratio of $\frac{h}{t}$ are two important non-dimensional parameters that describe the slenderness and aspect ratio of the rectangular cantilever beam. We simplify the elastic buckling equation including $\frac{t}{l}$ and $\frac{h}{t}$, which gives

$$P_{cb} = 0.669 \left(\frac{t}{l}\right)^2 (th)E \sqrt{\frac{1 - 0.63/\left(\frac{h}{t}\right)}{2(1+\nu)}} \quad 5.8$$

In order to capture the nature of the structure behaviors, we adapt the load for yield and collapse formulate to include $\frac{t}{l}$ and $\frac{h}{t}$ ratios. This gives

$$\frac{P_y}{\sigma_y A} = \frac{1}{6} \left(\frac{t}{l}\right) \left(\frac{h}{t}\right) \quad 5.9$$

$$\frac{P_c}{\sigma_y A} = \frac{1}{4} \left(\frac{t}{l}\right) \left(\frac{h}{t}\right) \quad 5.10$$

The elastic buckling load also can be re-stated as

$$\frac{P_{cb}}{\sigma_y A} = 0.669 \left(\frac{t}{l}\right)^2 \frac{E}{\sigma_y} \sqrt{\frac{1 - 0.63/\left(\frac{h}{t}\right)}{2(1+\nu)}} \quad 5.11$$

$$\text{let } t' = \frac{t}{l} \quad 5.12$$

$$h' = \frac{h}{t} \quad 5.13$$

substitute Equation 5.12, 5.13 into Equation 5.9, 5.10, and 5.11. we have

$$\frac{P_y}{\sigma_y A} = \frac{1}{6} t' h' \quad 5.14$$

$$\frac{P_c}{\sigma_y A} = \frac{1}{4} t' h' \quad 5.15$$

$$\frac{P_{cb}}{\sigma_y A} = 0.669 t'^2 \frac{E}{\sigma_y} \sqrt{\frac{(1 - 0.63/h')}{2(1 + \nu)}} \quad 5.16$$

The yield stress σ_y can be treated as a constant. If we set the rectangular section area as

A, then

$$P_t = \sigma_y A \quad 5.17$$

P_t load to cause axial yield (axial collapse, max possible of any case)

$$P_y^* = \frac{P_y}{P_t} \quad 5.18$$

$$P_c^* = \frac{P_c}{P_t} \quad 5.19$$

$$P_{cb}^* = \frac{P_{cb}}{P_t} \quad 5.20$$

$$P_y^* = \frac{1}{6} t' h' \quad 5.21$$

$$P_c^* = \frac{1}{4} t' h' \quad 5.22$$

$$P_{cr}^* = 0.669t'^2 \frac{E}{\sigma_y} \sqrt{\frac{(1-0.63/h')}{2(1+\nu)}} \quad 5.23$$

In order to understand the overall behavior of the cantilever beam, we should find the boundary of elastic buckling and initial yielding, and the boundary of plastic buckling and plastic hinge collapse, which are defined by non-dimensional parameters t' and h' .

From Equation 5.21 and 5.23, we can define the boundary of elastic buckling and initial yielding of cantilever beam by

$$\frac{1}{6}t'h' = 0.669t'^2 \frac{E}{\sigma_y} \sqrt{\frac{(1-0.63/h')}{2(1+\nu)}} \quad 5.24$$

$$t' = 0.2491 \frac{h'}{\frac{E}{\sigma_y} \sqrt{\frac{(1-0.63/h')}{2(1+\nu)}}} \quad 5.25$$

From Equation 5.22 and 5.23, we can define the virtual boundary of elastic buckling and plastic collapse of cantilever beam by

$$\frac{1}{4}t'h' = 0.669t'^2 \frac{E}{\sigma_y} \sqrt{\frac{(1-0.63/h')}{2(1+\nu)}} \quad 5.26$$

$$t' = 0.3737 \frac{h'}{\frac{E}{\sigma_y} \sqrt{\frac{(1-0.63/h')}{2(1+\nu)}}} \quad 5.27$$

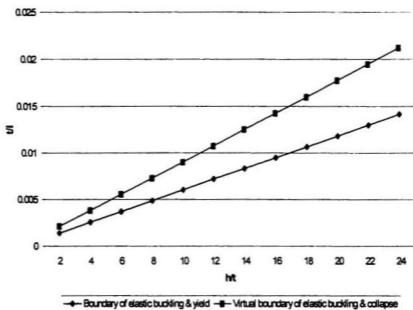
Equation 5.27 defines a virtual boundary of elastic buckling because in real practice, when the load exceeds the yield load, the stability equation established for the elastic

buckling is invalid. Nevertheless it, to some extent, provides us with useful hints for the boundary of plastic buckling and the collapse.

Table 5.1 Analytical Boundaries

Yield stress 3.00E+08
 Young's modulus 2.07E+11
 Poisson ratio 0.3

ν/l	h/t											
	2	4	6	8	10	12	14	16	18	20	22	24
ν/l for elastic buckling & yield, Eqn 5.25	0.00141	0.00254	0.00399	0.00485	0.00601	0.00718	0.00834	0.0095	0.01067	0.01183	0.01299	0.01416
ν/l for elastic buckling & collapse, Eqn 5.27	0.00211	0.00381	0.00554	0.00728	0.00902	0.01077	0.01251	0.01426	0.016	0.01775	0.01949	0.02124



5.2.2 Boundary of Plastic Buckling and Plastic Hinge Collapse

To determine boundary of plastic buckling and collapse, finite element analysis is applied. The behavior of the cantilever beam is related to t/l and h/t . If we set the length of a cantilever beam to 1 m, the thickness t and height h can be determined by two non-dimensional parameter t/l and h/t . Table 5.1 shows the cases studied by the finite element plastic buckling analysis.

Table 5.2 Grid of cases examined by nonlinear F.E. analysis

If we set $l=1\text{m}$, then w and h will be determined by ratios of h/t and t/l . Values in the table are the thickness t , height h									
t/l	h/t								
	5	5.5	6	6.5	7	7.5	8	8.5	9
t	h								
0.020	0.100	0.110	0.120	0.130	0.140	0.150	0.160	0.170	0.180
0.018	0.090	0.099	0.108	0.117	0.126	0.135	0.144	0.153	0.162
0.016	0.080	0.088	0.096	0.104	0.112	0.120	0.128	0.136	0.144
0.014	0.070	0.077	0.084	0.091	0.098	0.105	0.112	0.119	0.126
0.012	0.060	0.066	0.072	0.078	0.084	0.090	0.096	0.102	0.108
0.010	0.050	0.055	0.060	0.065	0.070	0.075	0.080	0.085	0.090
0.008	0.040	0.044	0.048	0.052	0.056	0.060	0.064	0.068	0.072
t/l	h/t								
	9.5	10	12	14	16	18	20	22	24
t	h								
0.020	0.190	0.200	0.240	0.280	0.320	0.360	0.400	0.440	0.480
0.018	0.171	0.180	0.216	0.252	0.288	0.324	0.360	0.396	0.432
0.016	0.152	0.160	0.192	0.224	0.256	0.288	0.320	0.352	0.384
0.014	0.133	0.140	0.168	0.196	0.224	0.252	0.280	0.308	0.336
0.012	0.114	0.120	0.144	0.168	0.192	0.216	0.240	0.264	0.288
0.010	0.095	0.100	0.120	0.140	0.160	0.180	0.200	0.220	0.240
0.008	0.076	0.080	0.096	0.112	0.128	0.144	0.160	0.176	0.192

In order to find the boundary of plastic buckling and the collapse of cantilever beam, nonlinear plastic buckling analysis was executed in each grid point in Table 5.2. After

running the ANSYS program at each grid point, we obtain the following plots: force – vertical deflection on the center of the free-end of cantilever beam; lateral deflection – vertical deflection of the center of the free-end of cantilever beam; the undeformed shape and deformed shape of the buckling load; and the von Mises stress contour of the buckled shape.

The force vs. vertical deflection of the center of the free-end of the cantilever beam will give us information to determine the plastic buckling force. Von Mises stress contour shows the stress distribution on the whole beam.

5.2.3 Procedure for Analysis of a Specific Case

In order to describe the typical procedure, we take the grid point on Table 5.2 $t/l=0.018$, $h/t=18$ to show whole analysis procedure.

First, we use the ANSYS solution program (Appendix A), for parameters t , h and l for the case. The ANSYS program is run in batch mode. In this step, the main task is to set up the geometric model, apply boundary conditions, and get the results for the all load substeps.

Second, we run the ANSYS program postprocessor (Appendix C), plot out graphical results: the Force vs. displacement on the center point of free end (window 1 in Figure 5.2), in which the x axis is displacement (m) and the y axis is the applied force (N). The lateral displacement vs. vertical displacement on the center point of free end (window 2

in Figure 5.2), in which the x axis is the vertical displacement (m) and the y axis is the lateral displacement (m). The Von Mises stress of top center point of the fixed end (window 3 in Figure 5.2), in which the x axis is the displacement and y axis is the stress (Pa). The purpose here is to determine the instability point location and property of the unstable point (i.e. if it is plastic or not).

Third, we run the program to get the final graphical results (Appendix B). The reference line on Figure 5.2 shows the instability time (normal to vertical displacement applied at free end). We set time for the instability point to plot out the deformed shape and stress contours. The Force vs. displacement and lateral displacement vs. vertical displacement are also included (See Figure 5.14).

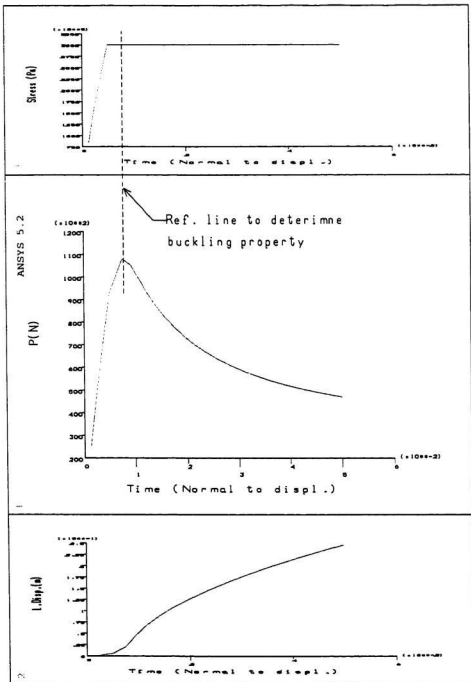


Figure 5.2 Pre-postprocessor result for $t/l=0.018$, $h/t=16$

5.3 Finite element analysis results

5.3.1 ANSYS Results for Plastic Buckling and Plastic Hinge

Collapse Boundary

The figures following Table 5.3 show the graphical results to find the boundary of plastic buckling and collapse.

As to determine boundary of plastic buckling and collapse, there is no analytical result. Cases study is essential to find boundary points. Figure 5.3 to Figure 5.25 are small portion of results of all cases has been studied, these figures are grouped by the ratio h/t from 8 to 24. And for each h/t value, less than 4 cases are presented to define the point on the boundary of plastic buckling and collapse.

Table 5.3 Comparing P_c , P_y , unstable load

If we set $l=1m$, then w and h will be determined by ratios of h/t and l/t										
Yield stress		3E+08 Pa								
l/t	h/t									
	6	8	10	12	14	16	18	20	22	24
$P_c(N)$										
0.020	21600	38400	60000	86400	117600	153600	194400	240000	290400	345600
0.018	15746	27994	43740	62986	85730	111974	141718	174960	211702	251942
0.016	11059	19661	30720	44237	60211	78643	99533	122880	148685	176947
0.014	7409	13171	20580	29635	40337	52685	66679	82320	99607	118541
0.012	4666	8294	12960	18662	25402	33178	41990	51840	62726	74650
0.010	2700	4800	7500	10800	14700	19200	24300	30000	36300	43200
0.008	1382	2458	3840	5530	7526	9830	12442	15360	18586	22118
$P_y(N)$										
0.020	14400	25600	40000	57600	78400	102400	129600	160000	193600	230400
0.018	10498	18662	29160	41990	57154	74650	94478	116640	141134	167962
0.016	7373	13107	20480	29491	40141	52429	66355	81920	99123	117965
0.014	4939	8781	13720	19757	26891	35123	44453	54880	66405	79027
0.012	3110	5530	8640	12442	16934	22118	27994	34560	41818	49766
0.010	1800	3200	5000	7200	9800	12800	16200	20000	24200	28800
0.008	922	1638	2560	3686	5018	6554	8294	10240	12390	14746
Behavior										
0.020	collapse collapse collapse collapse									
0.018	collapse plas.buck plas.buck plas.buck collapse collapse collapse									
0.016	plas.buck plas.buck plas.buck plas.buck plas.buck plas.buck plas.buck plas.buck									
0.014	collapse plas.buck plas.buck plas.buck etas.buck									
0.012	plas.buck									
0.010	collapse plas.buck									
0.008	collapse collapse									
Unstable load(N)										
0.020	115000 150000 160000 165000									
0.018	62500 82500 108000 125000 138000 140000									
0.016	43000 58000 74500 85000 100000 130000 120000									
0.014	20500 28000 38500 46000 75000									
0.012	12500									
0.010	4800 7300									
0.008	1300 2400									

ANSYS 5.2
 JUL 13 1998
 14:36:13
 PLOT NO. 1

WIND=2
 XV =1
 YV =1
 ZV =1
 DIST= .393157
 XF = .004155
 YF = .007036
 ZF = .501171
 Z-BUFFER

EDGE 267326
 .349E+07
 .671E+07
 .993E+07
 .132E+08
 .164E+08
 .196E+08
 .228E+08
 .260E+08
 .293E+08

POST26
 POST26

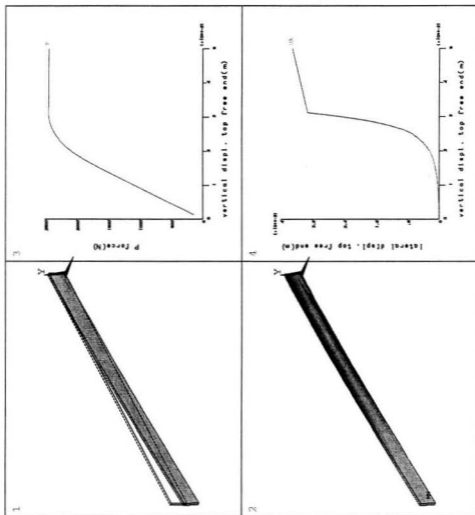


Figure 5.3 Finite element result for $t/l=0.008$, $h/t=8$

ANSYS 5.2
 JUL 11 1998
 20:19:39
 PLOT NO. 1

WIND=2
 XV =1
 YV =1
 ZV =1
 DIST=.397616
 XF =.00763
 YF =.045243
 ZF =.502525
 Z-BUFFER
 EDGE 315542
 .809E+07
 .159E+08
 .236E+08
 .314E+08
 .392E+08
 .470E+08
 .547E+08
 .625E+08
 .703E+08

POST26
 POST26

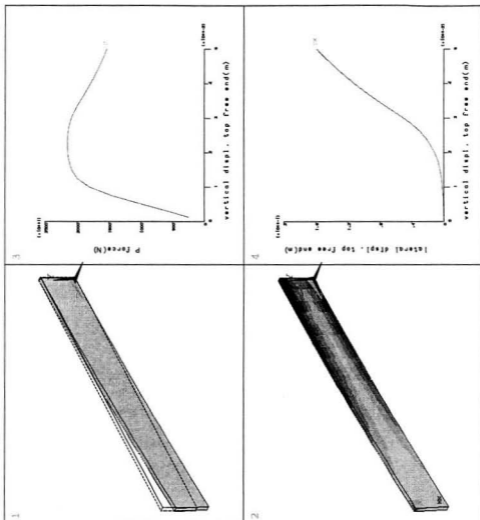


Figure 5.4 Finite element result for $t/l=0.014$, $h/t=10$

ANSYS 5.2
 JUL 12 1998
 16:59:28
 PLOT NO. 1

WIND=2
 XV =1
 YV =1
 ZV =1
 DIST=.396284
 XF =.006796
 YF =.035173
 ZF =.502169
 Z-BUFFER

EDGE
 550221
 .109E+08
 .213E+08
 .316E+08
 .420E+08
 .523E+08
 .627E+08
 .730E+08
 .834E+08
 .937E+08

POST26
 POST26

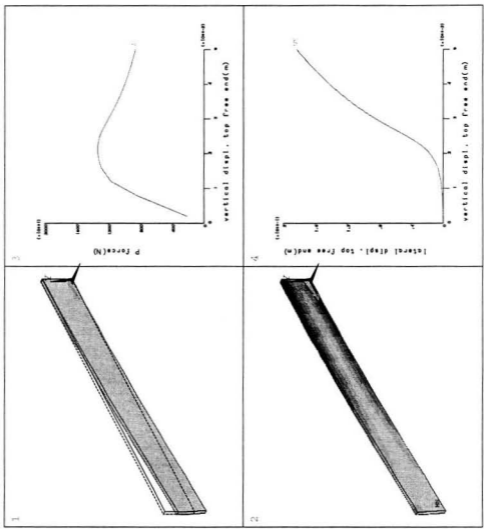


Figure 5.5 Finite element result for $t/l=0.012$, $h/t=10$

ANSYS 5.2
 JUL 10 1998
 14:31:42
 PLOT NO. 1

WIND=2
 XV = 1
 YV = 1
 ZV = 1
 DIST = .402319
 XF = .010516
 YF = .083822
 ZF = .503791
 Z-BUFFER
 EDGE 363828
 .129E+08
 .254E+08
 .379E+08
 .504E+08
 .630E+08
 .755E+08
 .880E+08
 .101E+09
 .113E+09

POST26
 POST26

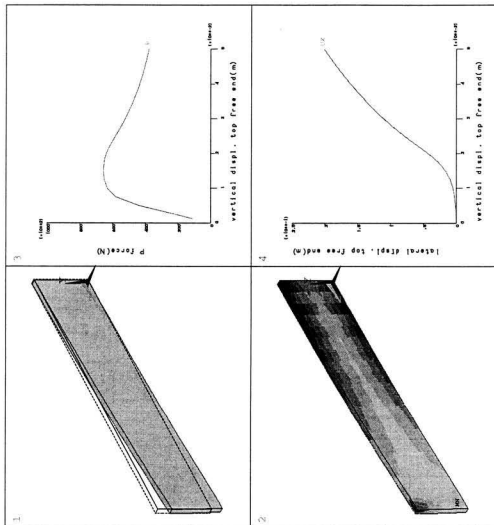


Figure 5.6 Finite element result for $t/l=0.018$, $h/t=12$

ANSYS 5.2
 JUL 10 1998
 13:59:53
 PLOT NO. 1

WIND=2
 XV =1
 YV =1
 ZV =1
 DIST=.400571
 XF =.009384
 YF =.071602
 ZF =.50341
 Z-BUFFER
 EDGE 368494
 .113E+08
 .222E+08
 .331E+08
 .440E+08
 .549E+08
 .658E+08
 .767E+08
 .877E+08
 .986E+08

POST26
 POST26

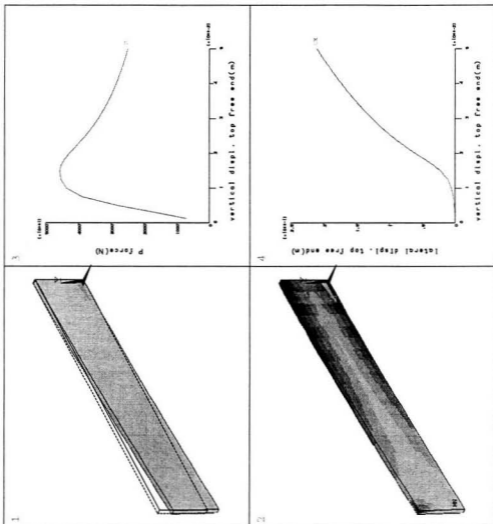


Figure 5.7 Finite element result for $t/l=0.016$, $h/t=12$

ANSYS 5.2
 JUL 10 1998
 10:10:15
 PLOT NO. 1

WIND=2
 XV =1
 XZ =1
 ZV =1
 DIST=.398871
 XF =.008236
 YF =.059423
 ZF =.503015
 Z-BUFFER
 EDGE 328803
 .966E+07
 .150E+08
 .283E+08
 .376E+08
 .470E+08
 .563E+08
 .656E+08
 .750E+08
 .843E+08

POST26
 POST26

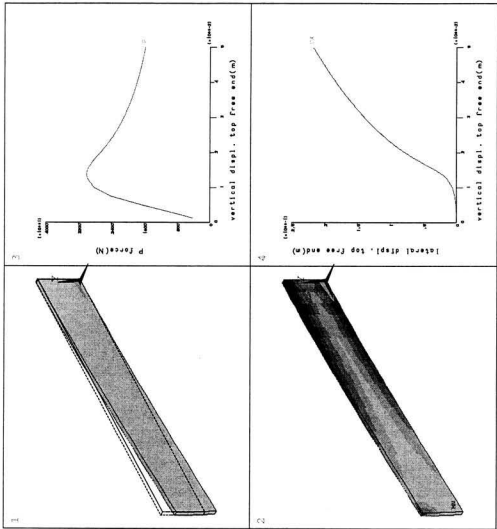


Figure 5.8 Finite element result for $t/l=0.014$, $h/t=12$

ANSYS 5.2
 JUL 9 1998
 11:12:14
 PLOT NO. 1

WIND=2
 XV =1
 YV =1
 ZV =1
 DIST=.406646
 XF =.012742
 YF =.11682
 ZF =.504731
 Z-BUFFER
 EDGE 447642
 .215E+08
 .425E+08
 .635E+08
 .846E+08
 .106E+09
 .127E+09
 .148E+09
 .169E+09
 .190E+09

POST26
 POST26

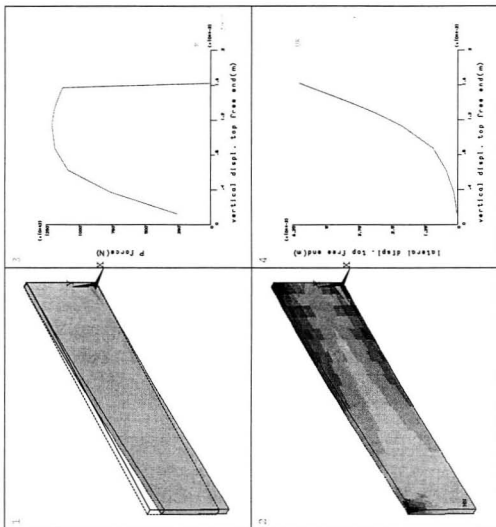


Figure 5.9 Finite element result for $t/l=0.020$, $h/t=14$

ANSYS 5.2
 JUL 8 1998
 12:01:00
 PLOT NO. 1

DSCA=38.463
 XV = 1
 YV = 1
 ZV = 1
 DIST= .404542
 XF = .011577
 YF = .102386
 ZF = .504343
 Z-BUFFER
 EDGE

372280
 .163E+08
 .320E+08
 .479E+08
 .637E+08
 .796E+08
 .954E+08
 .111E+09
 .127E+09
 .143E+09

POST26
 POST26

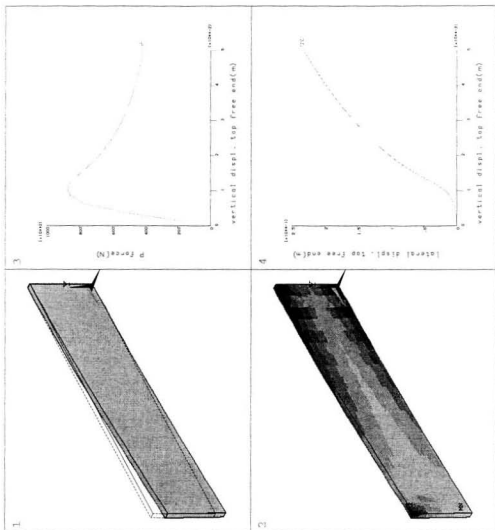


Figure 5.10 Finite element result for $t/l=0.018$, $h/t=14$

ANSYS 5.2
 JUL 10 1998
 14:09:47
 PLOT NO. 1

WIND=2
 XV =1
 YV =1
 ZV =1
 DIST=.402462
 XF =.01038
 YF =.088017
 ZF =.503927
 Z-BUFFER
 EDGE 382537
 .130E+08
 .257E+08
 .384E+08
 .510E+08
 .637E+08
 .763E+08
 .890E+08
 .102E+09
 .114E+09

POST26
 POST26

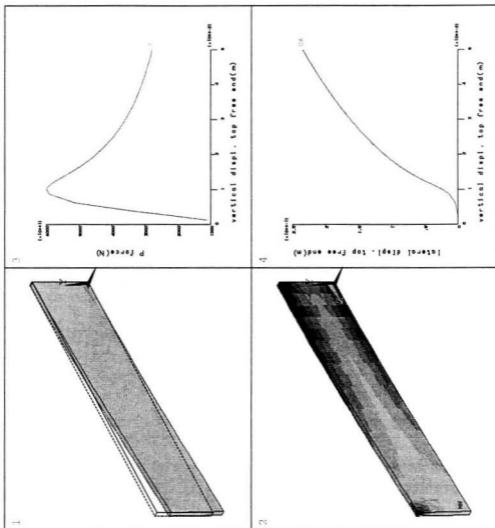


Figure 5.11 Finite element result for $t/l=0.016$, $h/t=14$

ANSYS 5.2
 JUL 10 1998
 13:14:40
 PLOT NO. 1

WIND=2
 XV = 1
 YV = 1
 ZV = 1
 DIST= .400442
 XF = .009137
 YF = .073715
 ZF = .503487
 Z-BUFFER
 EDGE
 420102
 .113E+08
 .221E+08
 .330E+08
 .438E+08
 .547E+08
 .655E+08
 .764E+08
 .872E+08
 .981E+08

POST26
 POST26

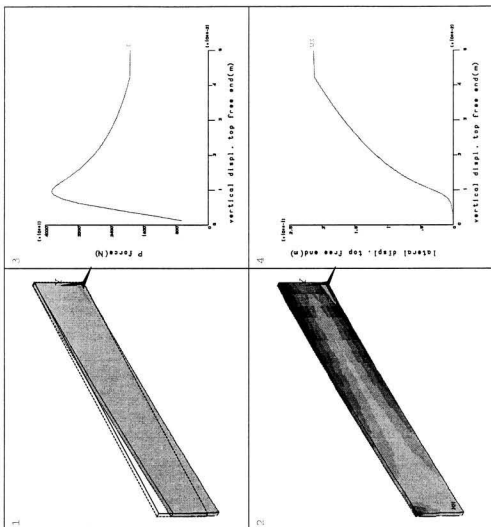


Figure 5.12 Finite element result for $t/l=0.014$, $h/t=14$

ANSYS 5.2
 JUL 9 1998
 11:20:04
 PLOT NO. 1

WIND=2
 XV =1
 YV =1
 ZV =1
 DIST=.409634
 XF =.014424
 YF =.137966
 ZF =.505187
 Z-BUFFER
 EDGE 474588
 .285E+08
 .565E+08
 .845E+08
 .112E+09
 .141E+09
 .169E+09
 .197E+09
 .225E+09
 .253E+09

POST26
 POST26

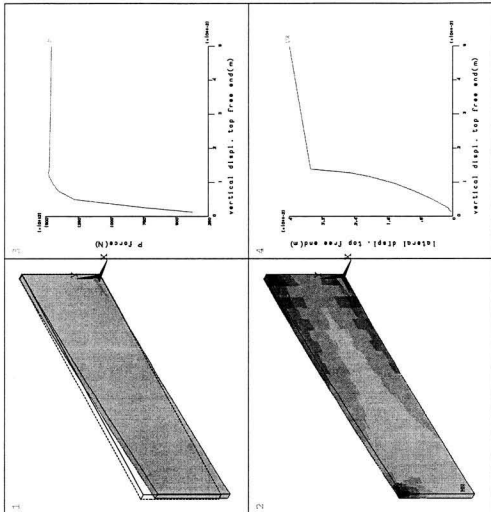


Figure 5.13 Finite element result for $t/l=0.020$, $h/t=16$

ANSYS 5.2
 JUL 8 1998
 20:13:50
 PLOT NO. 1

WIND=2
 XV =1
 YV =1
 ZV =1
 DIST=.407225
 XF =.013223
 YF =.121296
 ZF =.504807
 Z-BUFFER

EDGE
 454521
 .217E+08
 .430E+08
 .643E+08
 .856E+08
 .107E+09
 .128E+09
 .149E+09
 .171E+09
 .192E+09

POST26
 POST26

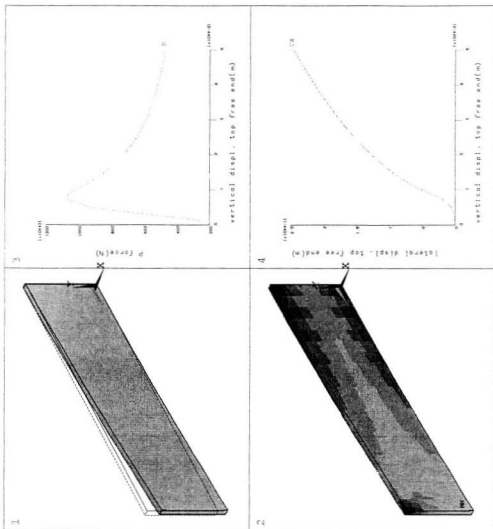


Figure 5.14 Finite element result for $t/l=0.018$, $h/t=16$

ANSYS 5.2
 JUL 8 1998
 21:17:50
 PLOT NO. 1

WIND=2
 XV =1
 YV =1
 ZV =1
 DIST=.404824
 XF =.011919
 YF =.104706
 ZF =.504385
 Z-BUFFER
 EDGE 478467
 .160E+08
 .315E+08
 .470E+08
 .626E+08
 .781E+08
 .936E+08
 .109E+09
 .125E+09
 .140E+09

POST26
 POST26

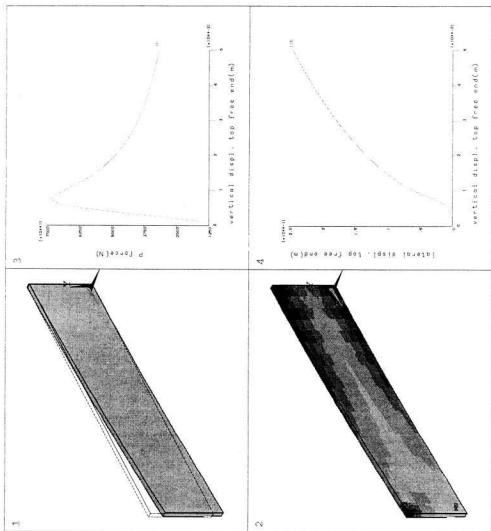


Figure 5.15 Finite element result for $t/l=0.016$, $h/t=16$

ANSYS 5.2
 JUL 12 1998
 17:35:41
 PLOT NO. 1

WIND=2
 XV =1
 YV =1
 ZV =1
 DIST= .402454
 XF = .010531
 YF = .088208
 ZF = .503972
 Z-BUFFER
 EDGE 443107
 .128E+08
 .251E+08
 .375E+08
 .499E+08
 .622E+08
 .746E+08
 .869E+08
 .993E+08
 .112E+09

POST26
 POST26

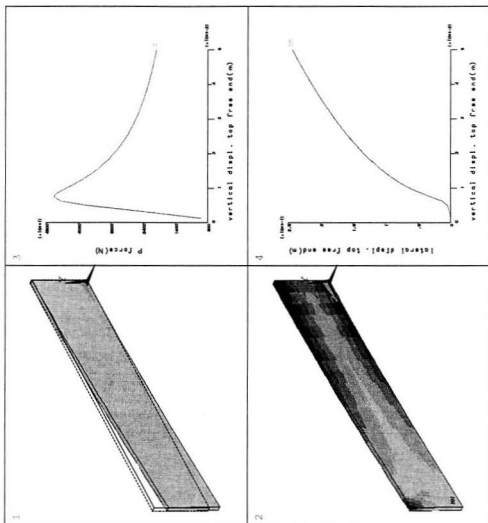


Figure 5.16 Finite element result for $t/l=0.014$, $h/t=16$

ANSYS 5.2
 JUL 9 1998
 11:28:00
 PLOT NO. 1

WIND=2
 XV =1
 YV =1
 ZV =1
 DIST=.418349
 XF =.016219
 YF =.159531
 ZF =.505481
 Z-BUFFER
 EDGE
 579305
 .362E+08
 .719E+08
 .108E+09
 .143E+09
 .179E+09
 .215E+09
 .250E+09
 .286E+09
 .322E+09

POST26
 POST26

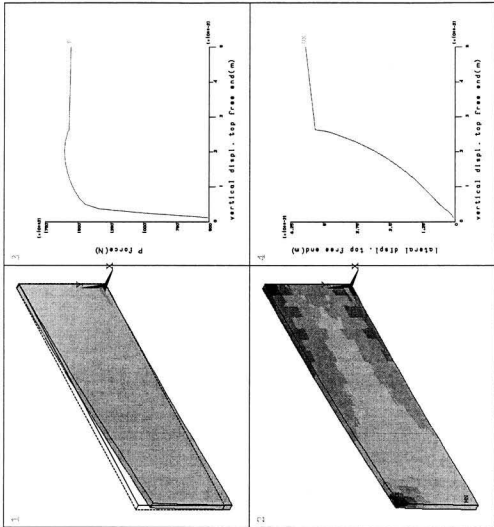


Figure 5.17 Finite element result for $t/l=0.020$, $h/t=18$

ANSYS 5.2
 JUL 8 1998
 20:28:33
 PLOT NO. 1

WIND=2
 XV =1
 YV =1
 ZV =1
 DIST= 410129
 XF = .015054
 YF = .140599
 ZF = .505143
 Z-BUFFER
 EDGE
 476258
 .279E+08
 .553E+08
 .827E+08
 .110E+09
 .137E+09
 .165E+09
 .192E+09
 .220E+09
 .247E+09

POST26
 POST26

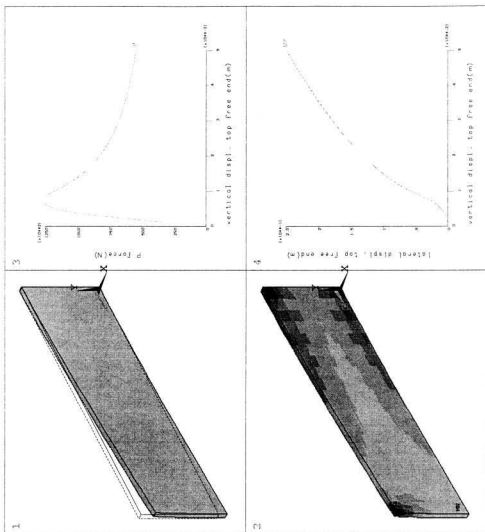


Figure 5.18 Finite element result for $t/l=0.018$, $h/t=18$

ANSYS 5.2
 JUL 8 1998
 21:34:45
 PLOT NO. 1

WIND=2
 XV =1
 YV =1
 ZV =1
 DIST= .407471
 XF = .013718
 YF = .121739
 ZF = .504747
 Z-BUFFER
 EDGE 437453
 .206E+08
 .408E+08
 .610E+08
 .811E+08
 .101E+09
 .121E+09
 .142E+09
 .162E+09
 .182E+09

POST26
 POST26

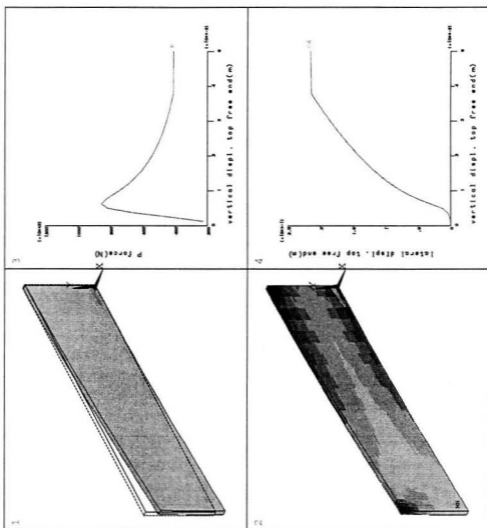


Figure 5.19 Finite element result for $t/l=0.016$, $h/t=18$

ANSYS 5.2
 JUL 16 1998
 14:11:14
 PLOT NO. 1

WIND=2
 XV =1
 YV =1
 ZV =1
 DIST=.417809
 XF =.017051
 YF =.160348
 ZF =.505304
 Z-BUFFER
 EDGE 629065
 .346E+08
 .687E+08
 .103E+09
 .137E+09
 .171E+09
 .205E+09
 .239E+09
 .273E+09
 .307E+09

POST26
 POST26

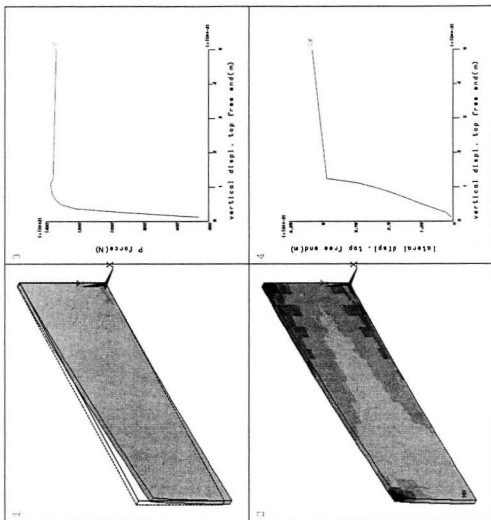


Figure 5.20 Finite element result for $t/l=0.018$, $h/t=20$

ANSYS 5.2
 JUL 8 1998
 21:52:20
 PLOT NO. 1

WIND=2
 XV =1
 YV =1
 ZV =1
 DIST= .41029
 XF = .015773
 YF = .139208
 ZF = .504969
 Z-BUFFER
 EDGE 480786
 .258E+08
 .531E+08
 .765E+08
 .102E+09
 .127E+09
 .152E+09
 .178E+09
 .203E+09
 .228E+09

POST26
 POST26

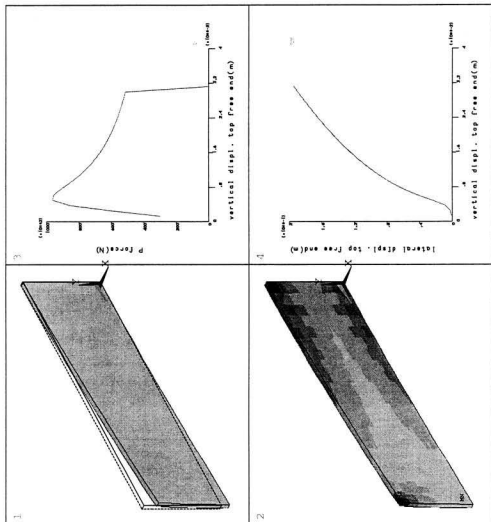


Figure 5.21 Finite element result for $t/l=0.016$, $h/t=20$

ANSYS 5.2
 JUL 16 1998
 14:26:46
 PLOT NO. 1

WIND=2
 XV = 1
 YV = 1
 ZV = 1
 DIST= .433481
 XF = .019475
 YF = .180667
 ZF = .505214
 Z-BUFFER
 EDGE 764100
 .418E+08
 .828E+08
 .124E+09
 .165E+09
 .206E+09
 .247E+09
 .288E+09
 .329E+09
 .370E+09

POST26
 POST26

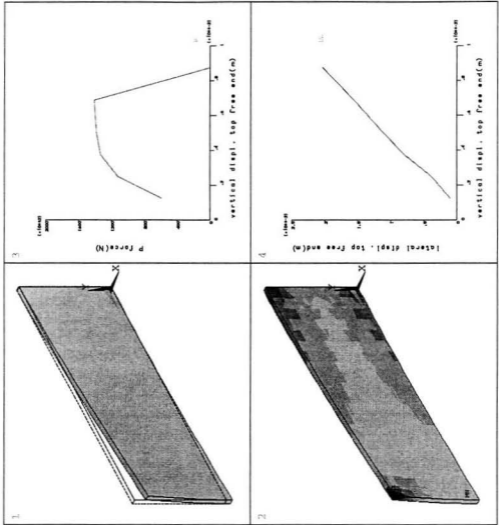


Figure 5.22 Finite element result for $t/l=0.018$, $h/t=22$

ANSYS 5.2
 JUL 9 1998
 09:51:40
 PLOT NO. 1

WIND=2
 XV =1
 YV =1
 ZV =1
 DIST=.413383
 XF =.018392
 YF =.157326
 ZF =.504962
 Z-BUFFER
 EDGE 622828
 .315E+08
 .624E+08
 .933E+08
 .124E+09
 .155E+09
 .186E+09
 .217E+09
 .248E+09
 .279E+09

POST26
 POST26

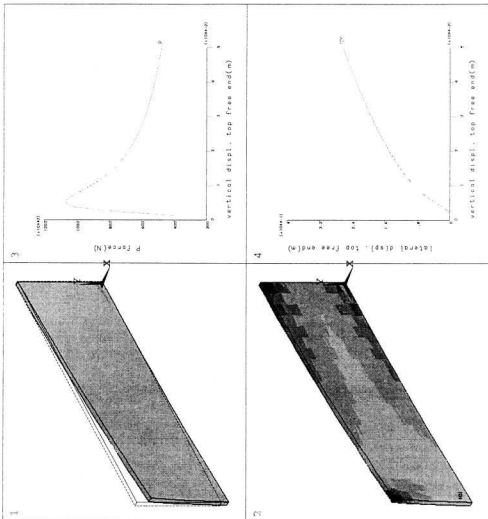


Figure 5.23 Finite element result for $t/l=0.016$, $h/t=22$

ANSYS 5.2
 JUL 9 1998
 10:06:21
 PLOT NO. 1

WIND=2
 XV =1
 YV =1
 ZV =1
 DIST=.427011
 XF =.020538
 YF =.175638
 ZF =.504781
 Z-BUFFER
 EDGE
 762770
 .375E+08
 .742E+08
 .111E+09
 .148E+09
 .164E+09
 .221E+09
 .258E+09
 .295E+09
 .331E+09

POST26
 POST26

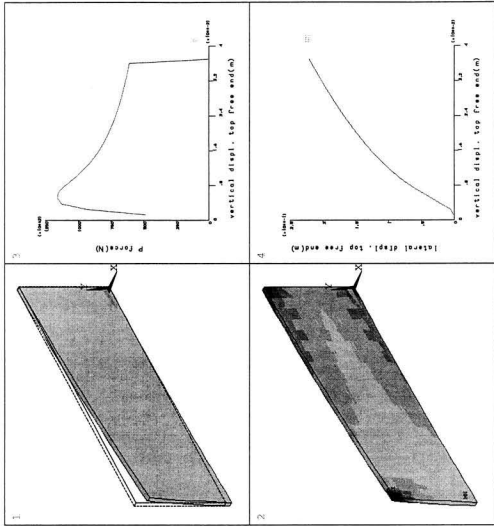


Figure 5.24 Finite element result for $t/l=0.016$, $h/t=24$

ANSYS 5.2
 JUL 12 1998
 17:14:25
 PLOT NO. 1

WIND=2
 XV = 1
 YV = 1
 ZV = 1
 DIST= .415144
 XF = .024809
 YF = .15492
 ZF = .503386
 Z-BUFFER
 EDGE
 .134E+07
 .434E+08
 .855E+08
 .128E+09
 .170E+09
 .212E+09
 .254E+09
 .296E+09
 .338E+09
 .380E+09

POST26
 POST26

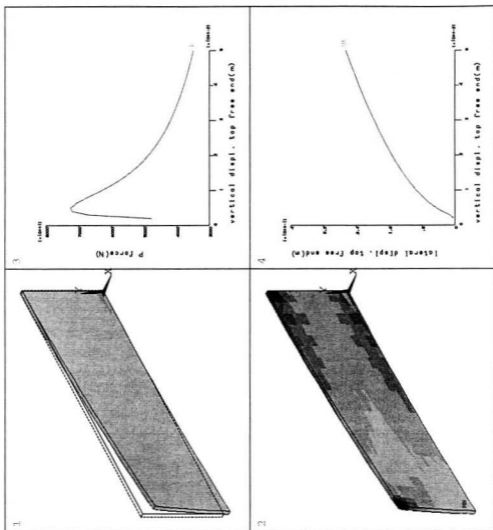


Figure 5.25 Finite element result for $t/l=0.014$, $h/t=24$

5.3.2 Overall Behavior of Cantilever Beam

In order to apply these finite element analysis results to convenient reference. The boundary of plastic buckling and yield and boundary of plastic buckling and collapse should be defined by non-dimensional ratios h/t and t/l .

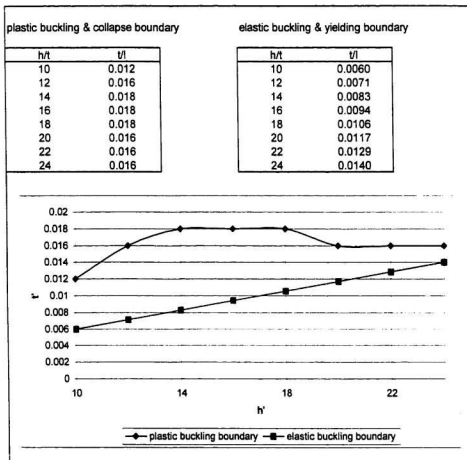
Table 5.4 summaries all related information presented in the graphical results. It includes the non-dimensional ratios h/t and t/l , and cantilever beam's behaviors for different ratios. The unstable loads for plastic buckling lay between the initial yield load and load of plastic hinge collapse. Also notice that, when h/t increase unstable load/ P_y , unstable load/ P_c are decreased. These infer that the cross section of a cantilever beam more slim, the structure more easier to have plastic buckling.

Table 5.4 Ratios of Unstable load/Pc, Unstableload/Py

If we set $t=1m$, then w and h will be determined by ratios of h/t and t/l										
Yield stress 3E+08 Pa										
t/l	h/t									
	6	8	10	12	14	16	18	20	22	24
Behavior										
0.020					collapse	collapse	collapse	collapse		
0.018					collapse	plas.buck	plas.buck	plas.buck	collapse	collapse
0.016					plas.buck	plas.buck	plas.buck	plas.buck	plas.buck	plas.buck
0.014					collapse	plas.buck	plas.buck	plas.buck		elas.buck
0.012					plas.buck					
0.010					collapse	plas.buck				
0.008	collapse	collapse								
Unstable load(N)										
0.020					115000	150000	160000	165000		
0.018					62500	82500	108000	125000	138000	145000
0.016					43000	58000	74500	85000	100000	110000
0.014					20500	28000	38500	46000		75000
0.012					12500					-
0.010					4800	7300				
0.008	1300	2400								
Unstable load/Pc										
0.020					0.9779	0.9766	0.8230	0.6875		
0.018					0.9923	0.9623	0.9645	0.8820	0.7888	0.6849
0.016					0.9720	0.9633	0.9473	0.8540	0.8138	0.7398
0.014					0.9961	0.9448	0.9545	0.8731		0.6327
0.012					0.9645					
0.010					1.0000	0.9733				
0.008	0.9404	0.9766								
Unstable load/Py										
0.020					1.4668	1.4648	1.2346	1.0313		
0.018					1.4884	1.4435	1.4468	1.3231	1.1831	1.0274
0.016					1.4581	1.4449	1.4210	1.2810	1.2207	1.1097
0.014					1.4942	1.4172	1.4317	1.3097		1.0173
0.012					1.4468					0.9490
0.010					0.9600	1.4600				
0.008	1.4106	1.4648								

The overall behavior of cantilever beam is summarized in Table 5.5. Boundary of elastic buckling and yield is derived from analytical method, while the boundary of plastic buckling and plastic hinge collapse is gotten from finite element analysis results.

Table 5.5 Overall Behavior of Cantilever Beam



5.3 Discussions

1. The plastic buckling and collapse boundary of cantilever beam is an irregular curve in the plane defined by two non-dimensional parameters h/t and t/l . The curve is above the boundary of elastic buckling and yielding, which is expected .

2. As shown in the diagram in Table 5.3, the overall behavior of the cantilever beam is defined by three regions. First the region below the boundary of elastic buckling and yielding is the elastic buckling region. The region between the boundary of plastic buckling and collapse and the boundary of elastic buckling and yielding is the plastic buckling region. The region above the boundary of plastic buckling and collapse is the collapse region.

3. Cantilever beams under vertical concentrated load at the free-end experience plastic buckling when ratio of h' is below 10 for any value of t' . Cantilever beam with ratio h/t (h') less than 10 will not experience plastic buckling for ratio t/l (t') range from 0.008 to 0.020. Ratio defines the slenderness of the rectangular cross section of cantilever beam. The plastic buckling will not happens if ratio of h/t is less than 10.

4. The slenderness of cantilever beam is the ratio t/l (t'). In the range of numerical study, plastic buckling usually happen when the ratio is less than 0.018, which means that if the cantilever beam is relatively short (ratio t/l bigger than the critical ratio), the cantilever beam will collapse by plastic hinge formation instead of buckling.

Chapter VI

CONCLUSIONS AND RECOMMENDATIONS

6.1 Conclusions

The finite element method can successfully be used for the plastic buckling analysis. The finite element method can include material nonlinearities and geometric nonlinearities, large deflection and large strain. In the solution procedure, in order to achieve a convergent solution for the nonlinear material and geometric nonlinearities, the Newton-Raphson method, an incremental method for the nonlinear system is applied. The finite element plastic buckling solution method provides a method for not only cantilever beam, but also for other structures with other types of material nonlinearity.

The thesis has set up two non-dimensional parameters as criteria for plastic buckling evaluation for the cantilever beam subjected to concentrated force at the center of the free-end. The two criteria parameters are ratio of thickness by length t/l and ratio of height by thickness h/t . The ratio of t/l defines the slenderness. Plastic buckling happens

when the ratio is less than about 0.018. The ratio h/w relates to the aspect ratio of the rectangular cross section. Plastic buckling happens when the ratio is bigger than 10 in studied range.

The overall behavior of cantilever beam under a concentrated load at the free-end is shown in the thesis. The diagram (in Table 5.3) is from the numerical results of finite element plastic buckling analysis and the analytical results of elastic buckling and yielding. There are three regions in the diagram. The elastic buckling region is under the boundary of elastic buckling and yielding. The plastic buckling region is between the boundary of plastic buckling and collapse and the boundary of elastic buckling and yielding; the region above the plastic buckling and collapse is collapse region.

The thesis also developed a general ANSYS model for plastic buckling analysis of cantilever beams subjected to concentrated force at the center of free-end. Any user can easily use the model to analyse a cantilever beam of different dimensions by changing the dimensions defined at the very beginning of the code.

6.2 Recommendations

Cross-section variations

This work is focused on plastic buckling behavior of cantilever beams, with rectangular cross sections. Cross-sections of the cantilever beam could be "I" section, "T" section or

another type of section. These sections are more complex than the rectangle. Finite element model should be set up for these sections to analyze plastic buckling load.

Different end condition

In this thesis, the beam is fixed at one end and free at the other. Other end conditions are expected to discuss such as fixed at two ends, pinned at two ends and continuous etc.

Different load conditions

Concentrated loads applied at the free-end of cantilever beam are studied in this work. In practice, the beam may be subjected to distributed loads along the length the beam, or have other types of load. It is worthwhile to study different load types.

Geometric imperfection

In the work, the model of cantilever beam is in perfect condition. There are no geometric imperfections in the model. Beams may have geometric imperfections or even gap in the structure. The effects of these imperfections may also be provided by finite element analysis.

Different material properties

Material property other than elastic-perfect plastic may be more realistic. Obviously, a multi-linear material curve will generate different load deflection response, hence providing different plastic buckling analysis solutions.

REFERENCES

- [1] Alexander Chajes, Principles of Structure Stability Theory, p3-28, Prentice-Hall Inc. 1974
- [2] Mario Como and Antonio Grimaldi, Theory of stability of continuous Elastic structure. "Preface", CRC Press Inc., 1995
- [3] W. C. Rheinbolt and E.Riks "Solution techniques for nonlinear finite element equations", State-of-art Surveys on Finite Element Technology, Edited by Ahmed K. Noor and Wakter D. Pilkey, p183-224, ASME, 1983
- [4] Kitipornchai Sritawat and Nicholas S. Trahair, "Buckling of inelastic I-Beam under moment gradient", Journal of the Structure Division, p991-1004, May 1975. ASCE
- [5] Mohamed H. El-Zanaty, David W. Murray, "Nonlinear finite element analysis of steel frames", Journal of the Structural Engineering, p353-68, Vol.109, ASCE
- [6] Dux Peter F. and Sritawat Kitipornchai, "Buckling approximations for inelastic beams". Journal of the Structural Engineering, p559-74. Vol.110, 1984, ASCE
- [7] Bradford Mark A., Peter E. Cuk, Marian A. Gizejowski and Trahair N.S., "Inelastic lateral buckling of beam-columns". Journal of the Structural Engineering, p2259-77, Vol.113 1987, ASCE
- [8] Trahair N. S. and S. Kitipornchai, "Buckling of inelastic I-beam under uniform moment", Journal of the Structural Division, p2551-66, 1972, ASCE
- [9] Doyle James F., "Matrix Analysis of Stability of Beams". Static and dynamic analysis of structures, p97-135, Kluwer Academic Publishers, 1991
- [10] Trahair N. S., "Inelastic buckling analysis", Flexural-Torsional Buckling of Structures, CRC Press, p245-276, 1993
- [11] F. Brezzi, "Behavior of finite of element solutions near a bifurcation point", Nonlinear Finite Element Analysis in Structure Mechanics, Editors W. Wunderlich, E.Stein, and K. J. Bathe, p109-121, Spring-Verlag, 1980
- [12] C. S. Desi and H. V. Phan, "Three-dimensional finite element analysis including material and geometric nonlinearities", Computational Methods in Nonlinear Mechanics, Edited by J. T. Oden, p205-25, North-Holland Publishing Company, 1979

- [13] Y. Yamada, T. Hirakwa, A. S. Wafi, "Analysis of large deformation and bifurcation in plasticity problems by the finite element method", Finite Elements in Nonlinear Mechanics Volume I, p393-412, Tapir Publishers, 1978
- [14] E. Riks, "An incremental approach to the solution of snapping and buckling problems", Int. J. Solids Structures, p529-51, Vol.15, 1979
- [15] S. L. Chan, "Geometric and material non-linear analysis of beam-columns and frames using the minimum residual displacement method", International Journal for Numerical Methods in Engineering, p2657-2669, Vol.26, 1988
- [16] S. L. Chan, "A Non-linear Numerical method for Accurate Determination of Limit and Bifurcation points", International Journal for Numerical Methods in Engineering, p2779-2790, Vol.36, 1993
- [17] St. Doltsinis, Nonlinear concepts in the analysis of solids and structures, Advances in computational Nonlinear Mechanics, Springer-Verlag, 1989
- [18] O. C. Zienkiewicz, "Visco-Plasticity, Plasticity, Creep and Visco-Plastic Flow", (Problems of small, large and continuing deformation), Lecture Notes in Mathematics, Computational Mechanics, International Conference on Computational Methods In Nonlinear Mechanics, Austin, Texas, Springer-Verlag, 1974
- [19] M. A. Crisfield, "Finite element analysis for combined material and geometric nonlinearities", Nonlinear Finite element Analysis In Structure Mechanics, Edited by W. Wunderlich, E. Stein, and K. -J. Bathe, p325-38, Springer-Verlag, 1980
- [20] Jacek J. Skrzypek, Plasticity and Creep, theory, Examples, and Problems, CRC Press, Inc., 1993
- [21] W.C. Rheiboldt and E. Riks, "Solution techniques for nonlinear finite element equations", State-of-the art surveys on Finite Element Technology, Edited by Ahmad K. Noor, walter D. Pildey, p183-225, 1983, ASME
- [22] N. P. G. Bergan, T. H. Soreide, "Solution of large displacement and instability problems using the current stiffness parameter", Finite Elements in Nonlinear Mechanics Volume II, p647-71, Tapir Publishers 1978,.
- [23] N.S. Trahair, Flexural-Torsional buckling of Structures, CRC Press Inc., 1993
- [24] Yuhshi Fukumoto, Structural Stability Design, Steel and Composite structures, Elsevier Science Inc. 1997

- [25] William A. Nash, "Plastic deformations of beams", Theory and Problems of Strength of Materials 3rdEd, p297 – p312, McGraw-Hill, INC. 1994
- [26] H. G. Allen and P. S. Bulson, Background to Buckling, p476, McGraw-Hill Book Co., 1980
- [27] Logan, Daryl L. A First course in the Finite Element Method 2nd Ed. PWS Publishing Company, Boston, 1992
- [28] Bathe, Klaus-Juren. Finite element procedures in engineering analysis Prentice-hall Inc. Englewood Cliffs, New Jersey, 1982
- [29] ANSYS user's Manual Revision 5.0 Volume I Procedures Swanson Analysis Systems, Inc.1992
- [30] ANSYS user's Manual Revision 5.0 Volume II Commands Swanson Analysis Systems, Inc.1992
- [31] ANSYS user's Manual Revision 5.0 Volume III Elements Swanson Analysis Systems, Inc.1992
- [32] ANSYS user's Manual Revision 5.0 Volume IV Theory Swanson Analysis Systems, Inc.1992
- [33] ANSYS Workbook Revision 5.2 Swanson Analysis Systems, Inc.1994
- [34] ANSYS user's Manual Examples supplement for Revision 5.1 Swanson Analysis Systems, Inc.1993

APPENDIX A

ANSYS52 General model and solution codes

```
/batch
!!!!!!!!!!!!!!!!!!!!!!!!!!!!!!!!!!!!!!!!!!!!!!!!!!!!!!!!!!!!!!!!!!!!!!!!!!!!!!
!!                                                                 !!
!!ANSYS CODE FOR PLASTIC BUCKLING ANALYSIS ON CANTILEVER BEAM!!
!!                                                                 !!
!!!!!!!!!!!!!!!!!!!!!!!!!!!!!!!!!!!!!!!!!!!!!!!!!!!!!!!!!!!!!!!!!!!!!!!!!!!!!!
!when the ANSYS program requires more heap space, the user can increase
the allocated space for
!ANSYS by ...%ansys52 -M 64      when start the ANSYS 64 indicates 64
mega bytes workspace

!this configuration command is not available in ANSYS52, user must
change the config file to do mem. configuration
!/config,nvpage,512 ! set maximum number of database pages in memory to
512

/com, the code is try to model the cantilever beam in general purpose,
!   i.e. it will be flexible to do various dimension analysis by only
modify
!   dimension parameters define at the beginning of the code;
furthermore the
!   material property is also changeable by modify adequate material
property
!   parameters in the code.
!   this section of code is mainly set up solid model
!   which includes the applied

!   boundary condition, both displacement and force applied on
expected model.

/COM,ANSYS REVISION  5.2                      19:58:56   01/27/1998
/view,1,1,1,1

/ang,1

/filnam,appdisp !job name
/title,plastic buckling analysis on cantilever beam

/units,si !set the unit system to metric system
```

```

!preprocessor
/!prep7
!define element types for setting up model
et,1,plane42
et,2,solid45

!define parameters for future use

!-----material properties
*set,ys,3.00e8 !yield strength (N/m.sqr)
*set,ym,2.07e11 !young's modulus ( N/m.sqr )
*set,poisson,0.3 !Poisson's ratio

!-----cantilever beam dimensions
*set,l,1 !the length of cantilever beam
*set,h,0.288 !the height of cantilever beam
*set,t,0.018!the thickness of cantilever beam

!-----define parameters for meshing
*set,nelem_t,6 !number of elements across thickness of beam
*set,nelem_h,8 !number of elements across the height of beam
*set,nelem_l,20!number of elements across length of beam

!-----the value of applied force on the free end
*set,f,5E4 !the central force applied on the free end (N)
*set,dx,0.05 !applied displacement on the center of top free end

!offset the center pointer with perturbation of an element thickness
!calculate the x value of applied force with one element thickness
perturbation
*set,vv,((nelem_t+2)*w/2/nelem_w)

!define material property as perfect plastic and with large-strain
ability
mp,ex,1,ym !define young's modulus for material 1
mp,nuxy,1,poisson !define Poisson's ratio for material 1
tb,biso,1,1,,0 !define the material property as bilinear isotropic
hardening(BISO)
! perfect plastic with large-strain ability
tbdata,1,ys,0 !yield stress ys; tangent modulus 0
tbplot,biso,1 !plot the material property

save !save database

!solid modeling

```

```

!----define keypoints
k,1,0,0,0 !keypoint 1
k,2,0,h,0 !keypoint 2
k,3,t,h,0 !keypoint 3
k,4,t,0,0 !keypoint 4
k,5,vv,h,0 !keypoint 5
k,6,vv,h,1 !keypoint 6 the force applied on

!----create straight lines
lstr,1,2 !create straight line from keypoint 1,2
lstr,2,3 !create straight line from keypoint 2,3
lstr,3,4 !create straight line from keypoint 3,4
lstr,4,1 !create straight line from keypoint 4,1
lstr,5,6 !create straight line from keypoint 5,6

save !save database

!----first create a 2-D meshed area for dragging to form the 3-D beam
al,1,2,3,4 !create area 1 from line 1,2,3,4

lesize,1,,,nelem_h,1, !number of division along line 1
lesize,3,,,nelem_h,1, !number of division along line 3
lesize,2,,,nelem_t,1, !number of division along line 2
lesize,4,,,nelem_t,1, !number of division along line 4
lesize,5,,,nelem_l,1, !number of division along line 5

type,1 !element type 1 for mesh on area 1
amesh,1 !mesh on area 1
eplot !plot elements

save !save database

!----drag to form 3-D beam
type,2 !switch to element type 2
mat,1 !material 1
esys,0 !element coordinate system ref. number
vdrag,1,,,,,5 !drag area 1 along line 5 to create 3-Dmesh
aclear,1 !delete no more useful plane element on area 1
eplot !plot element

save !save database

!apply loads
!----first apply displacement boundary condition
asel,s,,1 !select area 1 to form area component
cm,fixend,area !define selected area 1 as area component "fixed-end"

asel,s,,6
cm,freeend,area !define selected area 6 as area component "free-end"

```

```

save      !save database

cmsel,,fixend !select component "fixed-end"
lsel,,ext    !select external lines on selected component area "fixed-
end"
nsl1,,1     !select all node on selected lines
d,all,all   !constrain all DOF on selected nodes
allsel      !restores full sets of all entities

save      !save database

FINISH

/solu      !begin solution session

antype,0   !analysis type, static

nlgeom,on  !large deformation turned on

!-----second apply the force on the top of free end

d,node(vv,h,1),uy,-dx !apply the force on the specific keypoint

nrop,auto  !newton-rahpson method program choose
time,dx    !time set norm to force
autos,on   !auto step turned on
nsubst,40,100,20 !substep 40, maximum 100,minium 20
kbc,0      !ramped load
ncnv,2     !terminates analysis but not program execution if the
solution fails
           to converge

outr,all,all !output all result for each substep to database file

save      !save the database

solve
save

finish

```

APPENDIX B

ANSYS52 Postprocessor codes I

```
/COM,ANSYS REVISION 5.2                21:49:05   04/09/1996

/show,test,grph  !redirect graphic results to test.grph

*set,bkload,.0078 !define the buckling displacement (normal to time)
RESUME,appdisp,db,,

/plopts,info,on

/plopts,title,off

/FLOPTS,LEG1,0
/plopts,leg2,0
/plopts,leg3,0

/window,1,ltop  !define window 1 left top
/window,2,lbot  !define window 1 left bottom

/window,3,rtop  !define window 1 right top
/window,4,rbot  !define window 1 right bottom

/view,1,-1,1,1
/view,2,-1,1,1
/view,3,0
/view,4,0

/POST1

SET, , ,1, ,bkload , !read in the result of time of buckling load

/edge,all,1
/plots,frame,on
/window,all,off

/plopts,leg1,0
/plopts,leg2,0
/plopts,leg3,0

/window,1,on
```

```

/view,1,1,1,1
PLDISP,2      !plot deformed shape with undeformed edge
/window,1,off
/noerase

/plopts,leg2,1
/plopts,leg3,1

/window,2,on
/view,2,1,1,1
PLESOL,S,EQV  !plot von Mises stress contour of the buckling shape
/window,2,off
/noerase

!!!!!!!!!!!!!!
/plopts,leg1,off
/plopts,leg2,off
/plopts,leg3,off
/POST26

RFORCE,6,node(vv,h,1),F,Y,
NSOL,7,node(vv,h,1),U,X,ux

ABS,2,6, , ,P, , ,1,      !define reaction force on the node displacement
applied
ABS,3,7, , ,UX, , ,1,    !define lateral displacement of the node
displacement applied

/window,3,on
/view,3,0

/axlab,x,vertical displ. top free end(m)

/axlab,y,P force(N)
PLVAR,2, , , , , , , , ,
/window,3,off
/noerase

/window,4,on
/view,4,0
/axlab,x,vertical displ. top free end(m)
/axlab,y,lateral displ. top free end(m)
PLVAR,3, , , , , , , , ,
/window,4,off
/noerase

finish

```

APPENDIX C

ANSYS52 Postprocessor codes II

```
/COM,ANSYS REVISION 5.2                21:49:05    04/09/1998

/show,newpre,grph

RESUME,appdisp,db,,

/plot,info,off

/plot,title,off

/window,1,-0.3325,1.0025,-1,1 !define window 1
/window,2,-1,-0.3325,-1,1    !define window 2
/window,3,1.0025,1.67,-1,1  !define window 2

/edge,all,1
/plots,frame,on
/window,all,off

/view,1,0
/view,2,0

/POST26

RFORCE,6,node(vv,h,1),F,Y,
NSOL,7,node(vv,h,1),U,X,ux

ABS,2,6,,P,,1, !define reaction force on the node displacement
applied
ABS,3,7,,UX,,1, !define lateral displacement of the node
displacement applied

/window,1,on
/view,1,0

/axlab,x,Time (Normal to displ.)
/axlab,y,P(N)
/ANG,1,-90.000000,ZS,1

PLVAR,2,,,,,,,,,,,,

/window,1,off
/noerase
```

